Available online at www.sciencedirect.com
SCIENCE DIRECT®
Journal of Solid State Chemistry 178 (2005) 2452–2474
JOURNAL OF SOLID STATE CHEMISTRY
www.elsevier.com/locate/jssc

Interpenetrating metal-organic and inorganic 3D networks: a computer-aided systematic investigation. Part II [1]. Analysis of the Inorganic Crystal Structure Database (ICSD)

I.A. Baburin[a], V.A. Blatov[a,*], L. Carlucci[b], G. Ciani[b], D.M. Proserpio[b,*]

[a]*Samara State University, Ac. Pavlov St. 1, 443011 Samara, Russia*
[b]*Dipartimento di Chimica Strutturale e Stereochimica Inorganica (DCSSI), Università di Milano, Via G. Venezian 21, 20133 Milano, Italy*

Received 3 March 2005; received in revised form 18 May 2005; accepted 25 May 2005
Available online 11 July 2005

Abstract

Interpenetration in metal-organic and inorganic networks has been investigated by a systematic analysis of the crystallographic structural databases. We have used a version of TOPOS (a package for multipurpose crystallochemical analysis) adapted for searching for interpenetration and based on the concept of Voronoi–Dirichlet polyhedra and on the representation of a crystal structure as a reduced finite graph. In this paper, we report comprehensive lists of interpenetrating inorganic 3D structures from the Inorganic Crystal Structure Database (ICSD), inclusive of 144 Collection Codes for equivalent interpenetrating nets, analyzed on the basis of their topologies. Distinct Classes, corresponding to the different modes in which individual identical motifs can interpenetrate, have been attributed to the entangled structures. Interpenetrating nets of different nature as well as interpenetrating H-bonded nets were also examined.
© 2005 Elsevier Inc. All rights reserved.

Keywords: Network topology; Interpenetration; Inorganic structures

1. Introduction

A great variety of interpenetrating networks and entangled extended arrays are currently produced within the *areas* of inorganic and coordination chemistry, especially due to the intensive search for new functional materials. The analysis and rationalization of all these species can be a difficult and time-consuming work because of their ever growing number and for their increasing structural complexity, as evidenced by the continuous finding of many types of entanglements of individual motifs, particularly in the field of crystal engineering of coordination polymers, or metal-organic frameworks (MOFs) [1,2]. 'Interpenetrating networks' [1,3] are nowadays the more numerous entangled arrays, that need for a classification of the topology of the individual nets [4–8], as well as of the 'topology of interpenetration' [1,3,9], presently a not well explored field of chemical topology, but of fundamental relevance in the perspective to establish useful relationships between structure and properties. This troublesome analysis, however, can be facilitated by means of some computer-aided procedure.

We have recently described the use of the TOPOS package [1,10] for the automatic investigation of interpenetrated 3D metal-organic architectures in the Cambridge Structural Database (CSD). The investigation has produced a comprehensive list of 301 Refcodes, showing a variety of topological types and interpenetration degrees, and has allowed to assign different classes depending on the interpenetration relations of the distinct nets. The file of interpenetrating networks produced by Batten (http://web.chem.monash.edu.au/

*Corresponding authors. Fax: +39 02 5831 4454.
E-mail addresses: blatov@ssu.samara.ru (V.A. Blatov), davide.proserpio@istm.cnr.it (D.M. Proserpio).

0022-4596/$ - see front matter © 2005 Elsevier Inc. All rights reserved.
doi:10.1016/j.jssc.2005.05.029

Department/Staff/Batten/Intptn.htm) [9] was very useful for checking and improving the TOPOS program; all the cases quoted therein and 49 additional examples were found automatically with our program.

We report here the results of the analysis of interpenetration of 3D nets in the Inorganic Crystal Structure Database (ICSD, release 2005/1 with 86308 entries). Moreover, we have included in this analysis also the search for H-bonded interpenetrating nets, thanks to a recent improvement of the package. The same classification previously introduced in Part I [1] has been applied also to these species and the peculiar features of interpenetration in these inorganic materials have been discussed and compared with those observed in metal-organic architectures.

2. Automatic searching for 3D interpenetration in ICSD with TOPOS

The theoretical approach to the network analysis with the TOPOS program, based on the concept of Voronoi–Dirichlet polyhedron (VDP) and on the description of a crystal structure as a 'reduced' (or 'labelled quotient') finite graph, as well as the computational method employed for searching for interpenetration in 3D networks, have been previously described [10].

Some recent improvements of TOPOS are the following ones:

(i) an analysis of H-bonds and construction of the relevant adjacency matrix as described later (when H atoms are not reported TOPOS finds their ideal locations);
(ii) a new extended list of more than 1000 reference nets classified according to the three letter designation proposed by O'Keeffe [6c, 6d, 6e, 11] (very useful, *inter alia*, also for the classification of non-interpenetrated networks);
(iii) calculation of size of minimum circuits (n_{min}) to which every independent graph edge (chemical bond) belongs. This parameter is useful to automatically separate cluster groups in augmented or decorated nets. Indeed, the links between clusters have greater n_{min} values than other graph edges;
(iv) advanced graphical interface. All the structural diagrams in this paper were produced with TOPOS.

The peculiar aspects of the investigation of inorganic structures with TOPOS are discussed later.

2.1. Output parameters and interpenetration classes

In order to characterize interpenetration *phenomena* TOPOS provides a set of interpenetration output parameters that were proven to be useful in the analysis of the CSD files. They are summarized here in Table 1.

The above descriptors have allowed us to classify each case according to three Classes and their Subclasses (see Tables 2 and 3). This is a crystallographic approach to the 'topology of interpenetration': the analysis of the crystal structures has evidenced distinct Classes corresponding to the different modes in which individual identical motifs can interpenetrate, that can be represented by the operations generating the overall array from a single net. Thus, Classes are defined independently from the network topology.

Class Ia is the largest one in both databases [12]. The minimum values for Z are a strict consequence of our definitions of the Classes. Odd numbers for Z are observed in Classes Ia and IIa only. In the second Class this is quite exceptional [none example in ICSD and only one in CSD (3-fold NIGLUK)].

An example of Class IIb has been observed for the first time in ICSD [Eglestonite (Collection code 71900), see later].

2.2. Methods for the analysis of net connectivity in ICSD [13]

The problem of a correct determination of crystal structure connectivity (or an adjacency matrix of corresponding infinite graph) is particularly typical for inorganic compounds. Coordination numbers of atoms often are fairly great and cannot be unambiguously determined due to intricacy of their coordination spheres. For instance, alkali metals or atoms with lone electron pairs usually have at least two coordination spheres with fuzzy boundaries [14]. Obviously, dealing with net topology, we need to specify what kind of interatomic bonds is taken into account. In other words, most of the crystal structures can be described at several *representation levels*; each level corresponds to a set of *criteria* determining the structure connectivity. In the general case many representation levels are possible; some of them can be chemically unreasonable, but show an interesting topology. Thus, sodium metaborate $Na_3B_3O_6$ (Collection code 15967) is an example of crystal structure with chemically unambiguous topology: both cations have well-determined and narrow coordination spheres (2.515–2.590 Å for seven Na–O bonds and 1.337–1.397 Å for three B–O bonds). At this representation level $Na_3B_3O_6$ consists of a single 3D net. However, if one considers only two shortest Na–O bonds, of length 2.515 Å, keeping all B–O bonds, the single net falls into four interpenetrated nets that belong to the very rare topological Class IIIa.

We could mention here also the numerous structures of the Zircon, $Zr(SiO_4)$, type (Sp.Gr. $I4_1/amd$, ca. 200 Collection codes) and of the Scheelite, $Ca(WO_4)$, type (Sp.Gr. $I4_1/a$, ca. 140 Collection codes). In both ABO_4

Table 1
Summary of the descriptors of interpenetration

Z—Total degree of interpenetration	Total number of 3D interpenetrating nets. It is the product of translational (Z_t), and non-translational (Z_n) interpenetration.
FIV—Full interpenetration vector	The shortest vector defining the direction along which *all* the interpenetrating nets exactly superimpose and that, applied $Z-1$ times to a single net, generates the whole entanglement.
TIV—Translation interpenetration vector	When translational ($Z_t > 1$) and non-translational ($Z_n > 1$) operations are present we called TIV the shortest vector that relates all the Z_t interpenetrating nets.
PIV—Partial interpenetration vectors	When there is no FIV or TIV but more than one translational operation, different partial interpenetration vectors (PIVs) relate subgroups of Z_p independent nets. PIVs could be of two kinds: Z_{it} for integral translations and Z_{ct} for centering translations.
FISE—Full interpenetration symmetry element	Single space group symmetry element that generates *all* Z equivalent interpenetrating nets. No translational operations relating the nets are present (no FIV, TIV or PIV). The only Z allowed are 2,3,4,6.
NISE—Non-translating interpenetration symmetry element	When $Z_t > 1$ (TIV is present) a NISE symmetry element can exist that generates all Z_n interpenetrating nets.
PISE—Partial interpenetration symmetry element	Any space group symmetry element that generates Z_s (two or more) equivalent interpenetrating nets (but not *all* Z_n nets). If $Z_s = Z_n$ PISE is equivalent to NISE ($Z_t > 1$) or to FISE ($Z_t = 1$)
PIC—Primitive interpenetration cell	Any cell that contains the same number of atoms for *each* individual (colored) net is an "interpenetration cell". Among the possible *minimum* volume interpenetration cells we select the PIC as the one based on the vectors between atoms of the same net. Thus, PIC can be considered as the minimum primitive crystallographic cell constructed with *one* of the nets, i.e., the primitive cell to be assigned to the structure if it contains a single network.
PICVR—PIC volume ratio	The ratio of the PIC volume (V_{PIC}) divided by the primitive unit cell volume (V_0), $PICVR = V_{PIC}/V_0$. PICVR is integer, greater than or equal to unity.

Table 2
Classes of interpenetration of equivalent nets

Class	Nets relationships	Z	PICVR	Sub-class	Interp. Vector	Symm. Elem.	Z symbol	ICSD	CSD
I	Only translations (integral or centering)	Z_t	$= Z$	Ia	FIV	None	Z_t	78	163
				Ib	PIV	None	$Z(\sum Z_{it} * \sum Z_{ct})$	0	6
II	Space group symmetry operations	Z_n	$= 1$	IIa	None	FISE	Z_n	63	109
				IIb	None	PISE	$Z(\prod Z_n)$	1	0
III	Translations + symmetry operations	$Z_t \times Z_n$	$= Z_t$	IIIa	TIV	NISE	$Z(Z_t{*}Z_n)$	2	13
				IIIb	PIV	NISE	$Z[(\sum Z_{it} * \sum Z_{ct}) * Z_n]$	0	1
				IIIc[a]	TIV	PISE	$Z[Z_t * \prod Z_n]$	0	0
				IIId[a]	PIV	PISE	$Z[(\sum Z_{it} * \sum Z_{ct}) * \prod Z_n]$	0	0

[a]Speculative and not (never?) yet observed classes.

Table 3
Allowed numbers of equivalent 3D nets in Classes of interpenetration

Class	Z_t	Z_n	Degree of interpenetration Z[a]	Z_{min}
Ia	Any integer $\geqslant 2$	1	Any integer $\geqslant 2$,[a]	2
Ib	[b]Any $\sum_i Z_{it} \times \sum_i Z_{ct}$	1	Integer $\geqslant 4$, possible values are 4, 8, 9, 12, 16 etc. (no prime integers)	4
IIa	1	2, 3, 4, 6[c]	Only 2, 3, 4, 6	2
IIb	1	4, 6, 8, 12, 16, 24, 48	Only 4, 6, 8, 12, 16, 24, 48	4
IIIa	Any integer $\geqslant 2$	2, 3, 4, 6[c]	Any product $Z_t \times Z_n$ (no prime integers)	4
IIIb	[b]Any $\sum_i Z_{it} \times \sum_i Z_{ct}$	2, 3, 4, 6[c]	Any product $Z_t \times Z_n$; possible values are 8, 12, 16, 24 etc. (no prime integers)	8
IIIc	Any integer $\geqslant 2$	4, 6, 8, 12, 16, 24, 48	Any product $Z_t \times Z_n$; possible values are 8, 12, 16, 18 etc. (even numbers only)	8
IIId	[b]Any $\sum_i Z_{it} \times \sum_i Z_{ct}$	4, 6, 8, 12, 16, 24, 48	Any product $Z_t \times Z_n$; possible values are 16, 24, 32 etc. (no prime integers)	16

[a]Prime numbers are allowed only in class Ia.
[b]This formula assumes $Z_p = 2$ for all PIVs, and fits to all known structures. More general formula and other details concerning PIVs will be discussed in a future paper.
[c]Any possible order of the symmetry element.

families the B atoms are 4-connected while the A atoms show 8-coordination with two sets of four equivalent A–O contacts. When both sets are considered a single net results, but discarding the slightly longer set a 2-fold interpenetrated diamondoid array of Class IIa, with alternating tetrahedral A and B nodes, can be obtained. Sometime it could be also useful to select ad-hoc interactions to describe complex structures as interpenetrated (see tennantite, helvite and others examples in Ref. [8])

Before searching for interpenetration in inorganic compounds, therefore, we should substantiate the representation levels to be considered. Since the number of compounds to be investigated was extremely large, we should choose a set of formal *criteria* for automatic determination of adjacency matrix at each level. Such *criteria* can effectively be found by using the parameters of atomic VDP [15]. The total number of direct neighbors for an atom is determined as the number of 'major' [16] VDP faces; then chemical bonds are selected by considering solid angles (Ω) of the faces. Some minimum value of solid angle (in percentage of 4π steradian) corresponds to the weakest bonds taken into account. Many recent investigations showed this approach to be valid and useful [15].

The following representation levels were considered in this study:

1. The *valence* level, where all valence bonds are taken into account, both strong and also relatively weak. For instance, both coordination spheres are considered for alkali metals. This level corresponds to a special *method of intersecting spheres* [17] that uses the concept of *radius of spherical domain* (R_{sd}), in addition to the atomic crystallochemical radius, to recognize chemical bonds. R_{sd} is equal to the radius of a sphere of VDP volume and can be considered as an effective atomic radius in a given crystal field. Each atom is represented by two spheres: internal (with Slater radius) and external (with R_{sd}). A valence interaction between two atoms is assumed if (i) they have a common 'major' VDP face, (ii) there are at least two intersections between their internal or external spheres, and (iii) the solid angle of the face is greater than some value, assumed equal to 5% for inorganic compounds [18]. When there is a single intersection (between external spheres) we will refer to the bond as *specific* (secondary); if no intersections are found the atoms could be involved only into *van der Waals* interactions.

2. The *strong valence* level, where weak interatomic contacts are ignored. The scheme of the method of intersecting spheres was also used to calculate the adjacency matrix, but only the VDP faces with large Ω were considered. Two different calculations were performed at this level: with $\Omega > 10\%$ and $\Omega > 12\%$. Some crystal structures (e.g., pyrochlore structure), being a single net at the valence level, become interpenetrated at this level.

3. The *classic* level, that mainly rests upon the traditional crystallochemical approach to determination of interatomic bonds. The (ii) and (iii) *criteria* of the method of intersecting spheres are replaced by the requirement for an interatomic distance to be shorter than the sum of Slater radii of contacting atoms increased by 0.3 Å.

4. The *metal-reduced* level, that is derived from the strong valence level by removing all alkali and alkaline-earth (Ca, Sr, Ba) metals.

5. The *non-metal-reduced* level, that is equivalent to the strong valence level without halogen atoms.

6. The *H bond* level, where hydrogen bonds are considered together with valence bonds. TOPOS selects the H bonds A-H$\cdots$B among the secondary interactions determined by the method of intersecting spheres, applying the following default geometrical *criteria*: (i) the H bond distance r(H$\cdots$B) is $\leqslant 2.5$ Å; (ii) the distance between the atoms separated by an H bond bridge r(A$\cdots$B) is $\leqslant 3.8$ Å; (iii) the A-H$\cdots$B angle is 120° or greater (A and B atoms are defined by the user and, in this work, they were chosen as O, N, S, and halogens). For B equal to Cl, Br, or I the maximum r(H$\cdots$B) and r(A$\cdots$B) values were increased by 0.2, 0.3, or 0.4 Å, respectively. The H bonds A-H$\leftrightarrow$H-B with disordered hydrogen atoms were also recognized.

Each structure graph at each representation level was analyzed using the TOPOS program package, specially improved to find and classify 3D interpenetration [1]. The algorithm of the analysis includes the following steps:

1. Correcting atomic coordinates in disordered structures. If disordered atoms (except hydrogens) were located close to each other (<1 Å by distance) they were replaced by a *pseudo*-atom at the centroid of the disordered group.

2. Calculating adjacency matrix at a given representation level.

3. Selecting all metal atoms (if any) as complexing centers, and determining composition and topology of all ligands. At this step 3D interpenetration in the *non-metal* part of the crystal structure was recognized, as, for instance, in many borates and tellurates.

4. Simplifying the adjacency matrix by contracting all finite ligands to the complexing centers and keeping connectivity of the structure.

5. Analyzing topology of the simplified graph, detecting and classifying 3D interpenetration in the *whole* structure.

Owing to such versatile consideration of each compound all known cases of 3D interpenetration in inorganic substances were recognized and a lot of new examples were found. However, it is practically impossible to enumerate all representation levels for all inorganic compounds. We have only considered from a chemical point of view the most valuable variants,

keeping in mind that an entanglement in a real crystal structure should first have clear physical meaning. At the same time, if one would consider some specific problems, e.g., crystal formation, other representation levels could be required. In this case an unexpected entanglement could be discovered, as in the above mentioned species $Na_3B_3O_6$.

3. Analysis of the results

Our systematic search for interpenetration of 3D inorganic networks in ICSD (2005/1) has produced a comprehensive list, including 144 Collection Codes of identical interpenetrating 3D structures. Also in this case, as for the analysis of CSD, the list of interpenetrating networks by Batten [9] was checked for assessing the ability of the TOPOS program in discovering interpenetration. We should mention here that in ICSD there are numerous re-determinations of the same structure (on the average each has been determined 1.4 times…) and in the references we will list all of them from the most recent publication.

The examples are listed in different tables, depending on the connectivity of the nodes and on the topological types classified, when available, with the three letter designation proposed by O'Keeffe [6c, 6d, 6e, 11]. The distribution of the 30 different topologies (see Fig. 1) confirms that the most common interpenetrating nets are the diamondoid nets (44.8%, including augmented diamond and supertetrahedral nets), the α-polonium nets (18.8%, including augmented and decorated α-Po) followed by the $SrSi_2$ nets (6.3%). The distribution observed here parallels the one found for MOF in CSD: 41.9% **dia**; 17.3% **pcu** and 7.6% **srs** [1]. Indeed, the large majority of interpenetrating nets show 'common' topological types [1,2a]. Some less common and new topologies, however, were also found, that will be described later in detail [11].

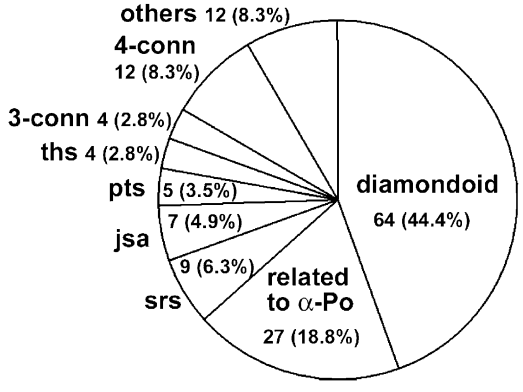

Fig. 1. Distribution of the topologies within the 144 structures.

3.1. General comments and comparisons

As already mentioned, the network description of inorganic species is complicated by the choice of the nodes, that often results even more arbitrary than for MOFs. What makes essentially different, moreover, the inorganic networks from the metal-organic ones is the length of the spacers connecting the nodes in the two cases. For inorganic species the links are mainly represented by direct interatomic covalent bonds or by one-atom or few-atom bridges. Thus the net edges are generally much shorter than in MOFs, that are built up with the use of long molecular spacers. This can have some relevant consequences on interpenetration. A survey of the results of our analysis, indeed, clearly shows some peculiar features: (i) the degree of interpenetration Z in almost limited to 2 (91%, only two cases 6-fold, one 4-fold and ten 3-fold) and (ii) consequently the Classes are almost completely restricted to Ia (54%) and IIa (44%).

Equivalent interpenetrating networks are listed in Tables 4–9. In many cases different structural determinations of the same species were performed in successive times, but we have reported in the tables a single Collection code, generally corresponding to the most recent crystallographic characterization. Non-identical nets and hydrogen-bonded nets will be considered later (Tables 10 and 11).

3.2. Three-connected interpenetrating nets

The species with this connectivity (17 cases) are reported in Table 4 [19]. The dominant topological type is that of $SrSi_2$ (**srs**) with 9 examples, followed by $ThSi_2$ (**ths**) with 4 examples. All nets but three have $Z = 2$.

Some cases are worth of a more detailed description. The structure of $Ta(PS_4)S_2$ (23284) illustrates the difficulty or arbitrariness of selection of the nodes. The Ta atoms are 3-connected and selecting them as nodes we obtain the **srs** topology. Alternatively, since Ta–Ta dinuclear moieties are present, choosing these units as nodes leads to diamondoid (**dia**) nets (see Fig. 2).

The srs family includes a group of four isomorphous compounds of formula MTe_3O_8 (M = Ti, Zr, Hf, Sn) in which the M metal cations are not comprised in the networks and the nodes are 3-connected O atoms. Also in the related case $K(GaTe_6O_{14})$ (280793) the K and Ga metal cations are not included in the nets, but these nets show a remarkable difference: we can recognize here two types of alternating nodes, 3-connected O and 3-connected Te_3O_6 triangles (see Fig. 3). We could define this net a hemi-decorated **srs**. Otherwise, considering the individual Te atoms as nodes, we obtain a new binodal 3-connected network of a topology having Schläfli symbol $(15^3)(3.15^2)_3$.

Table 4
Interpenetrating triconnected networks [19]

Collection code	Compound (Sp. Gr.)	Nodes[a]	Class	Z	PICVR	Non-Transl	Transl
$SrSi_2$ *uniform* (10^3)-*a* **srs**							
26521	α-Ag_3BO_3 (*R*32)	B, O 3-coor/Ag spacers	Ia	2	2		[001] (3.38 Å)
68386	$[(CO)_4Fe][Hg(SCN)]_2$ ($I4_1$/a)	Hg 3-conn/$Fe(CO)_4$ spacers	IIa	2	1	$\bar{1}$	
23284	$Ta(PS_4)S_2$ ($I4_1$/acd)	Ta oct/PS_4, S_2 spacers	IIa	2	1	$\bar{1}$	
9078	$HfTe_3O_8$ (*Ia* $\bar{3}$)	O 3-conn/Te spacers [Hf]	IIa	2	1	$\bar{1}$	
9077	$SnTe_3O_8$ (*Ia* $\bar{3}$)	O 3-conn/Te spacers [Sn]	IIa	2	1	$\bar{1}$	
98902[b]	$TiTe_3O_8$ (*Ia* $\bar{3}$) Winstanleyite	O 3-conn/Te spacers [Ti]	IIa	2	1	$\bar{1}$	
409713[b]	$ZrTe_3O_8$ (*Ia* $\bar{3}$)	O 3-conn/Te spacers [Zr]	IIa	2	1	$\bar{1}$	
280793	$K(GaTe_6O_{14})$ (*Pa* $\bar{3}$)	O, Te_3O_6 3-conn [K,Ga]	IIa	2	1	$\bar{1}$	
71900[b]	$(Hg_2)_3Cl_3O(OH)$ (*Ia* $\bar{3}$ *d*) Eglestonite	O/Hg_2 spacers [Cl]	IIb	4(2*2)	1	$\bar{1}$ 2-*axis*	
$ThSi_2$ *uniform* (10^3)-*b* **ths**							
72596	$CrP_3S_{9.238}$ (*Fddd*)	Cr 6-coor/P_2S_6 spacers	Ia	3	3		[0 1/2 1/2] (12.21 Å)
280333	$Ag_2(HgO_2)$ ($P4_32_12$)	O 3-conn/Hg, Ag spacers	Ia	3	3		[001] (8.42 Å)
34666[b]	$LiNa_2KFe_2Ti_2(Si_4O_{12})_2$ (*C*2/*c*) Neptunite	SiO_4 3-conn, [Li,Na,K,Fe,Ti]	IIa	2	1	$\bar{1}$	
281130	$Cs[AgZn(SCN)_4]$ (*C*2/*c*)	Ag 3-conn, Zn tet [Cs]	IIa	2	1	$\bar{1}$	
(4.12^2) **nbo-a**							
66547[b]	Ag(CNO) (*R* $\bar{3}$)	Ag, C 3-conn	Ia	2	2		[001] (5.73 Å)
Binodal uniform (8^3) **etc**, *Wells* (8^3)-c							
81997	$NaTi_2(PS_4)_3$ (*P*6*cc*)	Ti oct/PS_4 spacers, [Na]	IIa	2	1	2-*axis*	
Binodal uniform (10^3) $VS = [10_3.10_3.10_3][10.10_3.10_3]$							
32721	β-Ag_3BO_3 (*R* $\bar{3}$ *c*)	B, O 3-conn/Ag spacers	IIa	2	1	$\bar{1}$	
Pentanodal $(6.8.12)_4(6^2.10)$ $VS = [6.6.12_5][6.8.12_8](c_{10} = 495)$ $[6.8.12_6][6.8.12_8](c_{10} = 494)[6.8.12_7]$							
202397	$Ta_2(P_2S_{11})$ ($P2_1/c$)	Ta oct/PS_4, S_2 spacers	Ia	2	2		[100] (6.88 Å)

[a]Atoms or groups indicated in [ ] are not considered in the topological analysis.
[b]Multiple entry: different structure determinations with different codes.

Particularly interesting is the structure of the mineral Eglestonite, $(Hg_2)_3Cl_3O(OH)$ (71900), that was so far described by Wells [4] as a 4-fold interpenetrated srs net ignoring the chlorine anions. The nodes are 3-connected O atoms joined by Hg–Hg links (see Fig. 4). The structure is a solid racemate consisting of two pairs of enantiomeric nets. The two nets of the same handedness (i.e., the Blue and Yellow pair or the Green and Red one) are related between themselves a 2-fold axis while the nets of opposite chirality are related by an inversion center (the two symmetry operations are PISEs in our classification). Thus this species represents the unique example of the Class IIb, previously postulated by us [1]. However, a different classification is also possible considering that the O nodes of two enantiomeric pairs (Blue + Green or Yellow + Red) are bridged by [O···H···O] hydrogen bonds. A pair of nets, therefore, gives rise to a single 4-connected network, showing the topology of γ-silicon (Fig. 4, bottom right). The overall array results a 2-fold interpenetrated γ-Si (**gsi**) net belonging to Class IIa. The relation between two enatiomeric **srs** nets and **gsi** was firstly observed by O'Keeffe and Hyde in [6a].

Examples with other topologies are also of great interest. For instance, Ag(CNO) (66547) with 3-connected Ag and C nodes shows the augmented Nb oxide (**nbo-a**, see Fig. 5, left) topology, with $Ag_2(CNO)_2$ rings at the nodes of the NbO network (**nbo**). An augmented net is one in which the vertices of the original net are replaced by a polygon or polyhedron corresponding to the original coordination figure [6b,c,d, 11]. In $NaTi_2(PS_4)_3$ (81997), neglecting the Na cations, two interpenetrating binodal nets are present, showing the topology described by Wells as (8^3)-c [4] (**etc**), shown in Fig. 5, right.

Finally, we must mention here the case of the two forms of silver(I) orthoborate Ag_3BO_3 (both with 3-connected B and O nodes), one of which (26521) is 2-fold **srs** of Class Ia while the second (32721) is a novel binodal 10^3 net of Class IIa (see Fig. 6) [20]. It is worth noting that considering as nodes the whole 6-connected BO_3 units we obtain two interpenetrating α-Po (**pcu**) nets in both species.

3.3. Four-connected interpenetrating nets

Four-connected networks are reported in Tables 5–7. The family of interpenetrating diamondoid nets (**dia**, 42 Collection codes) is listed in Table 5 [21]. Only Class Ia (20 cases) and IIa (22 cases) are observed, with $Z = 2$ in 40 examples.

Table 5
Interpenetrating diamondoid (**dia**) networks [21]

Collection code	Compound (Sp. Gr.)	Nodes[a]	Class	Z	PICVR	Non-Transl	Transl
63281[b]	Cu_2O ($Pn\bar{3}m$) Cuprite	O tet, prototype	Ia	2	2		[100] (4.27 Å)
77651	Pd_2O ($Pn\bar{3}m$)	O tet, Cu_2O type	Ia	2	2		[100] (4.28 Å)
281041[b]	Ag_2O ($Pn\bar{3}m$)	O tet, Cu_2O type	Ia	2	2		[100] (4.73 Å)
28838	Pd_2O ($Pn\bar{3}m$)	O tet, Cu_2O type	Ia	2	2		[100] (5.38 Å)
77714	Zr_2O ($Pn\bar{3}m$)	O tet, Cu_2O type	Ia	2	2		[100] (5.09 Å)
78718	Au_2S ($Pn\bar{3}m$)	S tet, Cu_2O type	Ia	2	2		[100] (5.02 Å)
87215[b]	$Ag_{2-x}Au_xS$ ($Pn\bar{3}m$)	S tet, Cu_2O type	Ia	2	2		[100] (4.95 Å)
93725	$Be(CN)_2$ ($Pn\bar{3}m$)	Be tet	Ia	2	2		[100] (5.34 Å)
66938[b]	$Cd(CN)_2$ ($P\bar{4}3m$)	Cd tet	Ia	2	2		[100] (6.30 Å)
93726	$Mg(CN)_2$ ($Pn\bar{3}m$)	Mg tet	Ia	2	2		[100] (6.12 Å)
412317[b]	$Zn(CN)_2$ ($Pn\bar{3}m$)	Zn tet	Ia	2	2		[100] (5.91 Å)
93543	SiC_2N_4 ($Pn\bar{3}m$)	Si tet	Ia	2	2		[100] (6.19 Å)
77654	$Pt(IV)O_2$ ($Pn\bar{3}m$)	Pt tet	Ia	2	2		[100] (3.95 Å)
78986	$(NH_4)_3Cu_4Ho_2Br_{13}$ ($Pn\bar{3}$)	$Br(CuBr_3)_4$/Ho spacers	Ia	2	2		[100] (11.02 Å)
402503	$Rb_3Cu_4Tm_2Br_{13}$ ($Pn\bar{3}$)	$Br(CuBr_3)_4$/Tm spacers [Rb]	Ia	2	2		[100] (11.02 Å)
24541	$(NH_4)_5Ce[Ni(NO_2)_6]_2$ ($Pn\bar{3}$)	Ce 12-coor/Ni spacers	Ia	2	2		[100] (10.58 Å)
411179	$Ag(B(CN)_4)$ ($P\bar{4}3m$)	B tet, Ag tet	Ia	2	2		[100] (5.73 Å)
30854	$LiCo(CO)_4$ ($P\bar{4}3m$)	Co tet, Li tet	Ia	2	2		[100] (5.54 Å)
56730	$Ca(AlCl_4)_2$ ($I4_1/acd$)	Ca 8-coor/$AlCl_4$ spacers	IIa	2	1	$\bar{1}$	
56729	$Yb(AlCl_4)_2$ ($I4_1/acd$)	Yb 8-coor/$AlCl_4$ spacers	IIa	2	1	$\bar{1}$	
56743[b]	$Sr(AlCl_4)_2$ ($Pbca$)	Sr 8-coor/$AlCl_4$ spacers	IIa	2	1	$\bar{1}$	
77083[b]	$CsHSO_4$ ($I4_1/amd$)	Cs tet, S tet	IIa	2	1	$\bar{1}$	
62889[b]	$CsDSO_4$ ($I4_1/amd$)	Cs tet, S tet	IIa	2	1	$\bar{1}$	
51314	$LiAlB_2O_5$ ($C2/c$)	AlB_2O_3/O spacers [Li]	IIa	2	1	$\bar{1}$	
14361	CdB_4O_7 ($Pbca$)	B_4O_5/O spacers [Cd]	IIa	2	1	$\bar{1}$	
96560	CoB_4O_7 ($Pbca$)	B_4O_5/O spacers [Co]	IIa	2	1	$\bar{1}$	
281287	HgB_4O_7 ($Pbca$)	B_4O_5/O spacers [Hg]	IIa	2	1	$\bar{1}$	
9086[b]	ZnB_4O_7 ($Pbca$)	B_4O_5/O spacers [Zn]	IIa	2	1	$\bar{1}$	
6170	MnB_4O_7 ($Pbca$)	B_4O_5/O spacers [Mn]	IIa	2	1	$\bar{1}$	
34397	MgB_4O_7 ($Pbca$)	B_4O_5/O spacers [Mg]	IIa	2	1	$\bar{1}$	
65930[b]	$Li_2B_4O_7$ ($I4_1cd$) Diomignite	B_4O_5/O spacers [Li]	IIa	2	1	*c-glide*	
93836	CsB_5O_8 ($Pbca$)	B_5O_6/O spacers [Cs]	IIa	2	1	$\bar{1}$	
2712[b]	KB_5O_8 ($Pbca$)	B_5O_6/O spacers [K]	IIa	2	1	$\bar{1}$	
93838[b]	RbB_5O_8 ($Pbca$)	B_5O_6/O spacers [Rb]	IIa	2	1	$\bar{1}$	
50927	TlB_5O_8 ($Pbca$)	B_5O_6/O spacers [Tl]	IIa	2	1	$\bar{1}$	
2045	$Na_2B_6O_{10}$ ($P2_1/c$)	B_5O_6, B_4O_5/O spacers [Na]	IIa	2	1	$\bar{1}$	
98571[b]	$Ag_2B_8O_{13}$ ($P2_1/c$)	B_5O_6, B_3O_3/O spacers [Ag]	IIa	2	1	$\bar{1}$	
95870[b]	$Na_2B_8O_{13}$ ($P2_1/a$)	B_5O_6, B_3O_3/O spacers [Na]	IIa	2	1	$\bar{1}$	
26203	BaB_8O_{13} ($P4_122$)	B_5O_6, B_3O_3/O spacers [Ba]	IIa	2	1	2-*axis*	
279578	$Li_2(AlB_5O_{10})$ ($P2_1/c$)	B_5O_6, AlO_4 [Li]	IIa	2	1	$\bar{1}$	
67526	Ag_3CuS_2 ($I4_1/amd$) Jalpaite	$Ag_4Cu_2S_4$/Ag spacers	Ia[c]	3	3		[1/2 1/2 1/2](8.49 Å)
31360[b]	$CsCo(CO)_4$ ($I\bar{4}$)	Cs tet, Co tet	Ia	3	3		[001] (5.34 Å)

[a]Atoms or groups indicated in [ ] are not considered in the topological analysis.
[b]Multiple entry: different structure determinations with different codes.
[c]A case of translational interpenetration that does not show the "normal mode".

As previously stated [1], our categorization can be useful for the analysis of the so-called 'normal mode of interpenetration' in diamondoid nets [3d], whose typical aspect is that the nodes of all the Z independent nets are equally spaced along one of the 'ideal' 2-fold axes of the adamantanoid cage and each net is translated along this direction by $1/Z$ the cage height. This mode must be limited to Class Ia, but not all the interpenetrated diamondoid nets of this Class are 'normal'. A case of 'non-normal' interpenetration is that of the 3-fold **dia** Ag_3CuS_2 (67526), illustrated in Fig. 7, whose nodes are $Ag_4Cu_2S_4$ clusters.

A numerous group of 2-fold interpenetrated **dia** networks is that of anhydrous borates (and related compounds). In all these species the cations do not participate to the nets and the nodes consist of O-bridged borate units, like B_3O_3, B_4O_5 and B_5O_6 (see Fig. 8), either of a single type or (in four cases) of two different types. Nodes like these are also present in interpenetrating networks showing other topologies (see later).

Interpenetrating augmented and supertetrahedral diamondoid networks are reported in Table 6 [22], all having $Z = 2$ and belonging to Class IIa, but one. The

Table 6
Interpenetrating augmented and supertetrahedral diamond (**dia**) networks [22]

Collection code	Compound (Sp. Gr.)	Nodes[a]	Class	Z	PICVR	Transl/Non-Transl
Augmented diamond **dia-a** (*T*2)						
281482	$[Ir_4(CO)_8F_2](Sb_2F_{11})_2$ ($P\bar{4}n2$)	Ir cluster/Sb_2F_{11} spacers	Ia	2	2	[001] (9.53A)
78774[b]	$BeCl_2$ ($I4_1/acd$)	$[Be_4Cl_6]$ 4-conn/Cl spacers	IIa	2	1	$\bar{1}$
92587	BeI_2 ($I4_1/acd$)	$[Be_4I_6]$ 4-conn/I spacers	IIa	2	1	$\bar{1}$
30803	$ZnBr_2$ ($I4_1/acd$)	$[Zn_4Br_6]$ 4-conn/Br spacers	IIa	2	1	$\bar{1}$
2404	ZnI_2 ($I4_1/acd$)	$[Zn_4I_6]$ 4-conn/I spacers	IIa	2	1	$\bar{1}$
281134	HgI_2 ($I4_1/acd$)	$[Hg_4I_6]$ 4-conn/I spacers	IIa	2	1	$\bar{1}$
85527	GeS_2 ($I4_1/acd$)	$[Ge_4S_6]$ 4-conn/S spacers	IIa	2	1	$\bar{1}$
34607	$Be(NH_2)_2$ ($I4_1/acd$)	$[Be_4(NH_2)_6]$ 4-conn/NH_2 spacers	IIa	2	1	$\bar{1}$
16222	$Mg(NH_2)_2$ ($I4_1/acd$)	$[Mg_4(NH_2)_6]$ 4-conn/NH_2 spacers	IIa	2	1	$\bar{1}$
89582	$Mn(NH_2)_2$ ($I4_1/acd$)	$[Mn_4(NH_2)_6]$ 4-conn/NH_2 spacers	IIa	2	1	$\bar{1}$
89581	$Zn(NH_2)_2$ ($I4_1/acd$)	$[Zn_4(NH_2)_6]$ 4-conn/NH_2 spacers	IIa	2	1	$\bar{1}$
86016	$Ca_3Ga_2N_4$ ($I4_1/acd$)	$[Ga_4N_6]$ 4-conn/N spacers [Ca]	IIa	2	1	$\bar{1}$
73307	Na_2SnAs_2 ($I4_1/acd$)	$[Sn_4As_6]$ 4-conn/As spacers [Na]	IIa	2	1	$\bar{1}$
Supertetrahedral diamond						
73150	$Li_5(B_7S_{13})$ ($C2/c$)	T2 (B_4S_6), T3 ($B_{10}S_{16}$) 1:1/S spacers [Li]	IIa	2	1	$\bar{1}$
412579	$Na_{5.88}(B_{10}Se_{18})$ ($I4_1/acd$)	T3 ($B_{10}S_{16}$)/S spacers [Na]	IIa	2	1	$\bar{1}$
78993	$Na_6(B_{10}S_{18})$ ($I4_1/acd$)	T3 ($B_{10}S_{16}$)/S spacers [Na]	IIa	2	1	$\bar{1}$
33270	$Ag_6(B_{10}S_{18})$ ($C2/c$)	T3 ($B_{10}S_{16}$)/S spacers [Ag]	IIa	2	1	$\bar{1}$
69352	$Li_{9.8}(B_{10}S_{18})S_{1.9}$ ($C2/c$)	T3 ($B_{10}S_{16}$)/S spacers [Li]	IIa	2	1	$\bar{1}$
93107	$(Cd_4In_{16}S_{33})(H_2O)_{20}[(N_2C_4H_8)((NH_2)C_3H_6)_2]_{2.5}$ ($I4_1/acd$)	T4 ($Cd_4In_{16}S_{31}$)/S spacers	IIa	2	1	$\bar{1}$
93103	$(Zn_4In_{16}S_{33})[(N_2C_4H_8)((NH_2)C_3H_6)_2]$ ($I4_1/acd$)	T4 ($Zn_4In_{16}S_{31}$)/S spacers	IIa	2	1	$\bar{1}$
93104	$(Zn_4In_{16}S_{33})[(N_2C_4H_9)((NH_2)C_2H_4)]$ ($I4_1/acd$)	T4 ($Zn_4In_{16}S_{31}$)/S spacers	IIa	2	1	$\bar{1}$
281747	$(In_{2.39}Ge_{1.61}S_8)(H_2O)_{0.25}$ ($I4_1/acd$)	Pseudo T4 ($In_8Ge_8S_{30}$)/S spacers	IIa	2	1	$\bar{1}$

[a]Atoms or groups indicated in [ ] are not considered in the topological analysis.
[b]Multiple entry: different structure determinations with different codes.

augmented diamondoid nets (**dia-a**, 13 cases) show diamond (**dia**) nodes that are decorated by tetrahedra (T2). The case of the prototypical $BeCl_2$ (78774), that is comprised of Be_4Cl_6 adamantane cages as nodes, is illustrated in Fig. 9.

Nine examples of interpenetrating supertetrahedral networks are also known, showing the diamond network decorated by tetrahedra of higher order (T3 and T4). A case (73150) with mixed T2/T3 nodes is also known (see Fig. 10, top).

The non-diamondoid 4-connected nets are reported in Table 7 [23]. This long list comprises different uninodal and polynodal topologies. Seven uninodal types were found, four more common [$SrAl_2$ (**sra**), quartz (**qtz**), NbO (**nbo**) and $CdSO_4$ (**cds**)] and three less common [Gismondine (**gis**) and **lcv** (or **srs-e**), illustrated in Fig. 11, and **lvt**, shown in Fig. 12, left].

Two out of the three observed cases with the quartz (**qtz**) topology exhibit the highest Z value (6) observed in the ICSD. These two isomorphous species, *namely* $Co(Au(CN)_2)_2$ (41197) and $Zn(Au(CN)_2)_2$ (83675), contain six homochiral quartz nets and belong to Class IIIa; they can be described in an alternative way including in the list of bonds also the short aurophilic Au–Au contacts, that join three nets into a single one, as 2-fold (3,4)-connected net (Class IIa related by 2-axis) with Schläfli symbol $(9^2.10)_2(9^4.10^2)$.

The more numerous groups have polynodal network topologies. These include a net derived from **pcu** decorated with hexagons (**pcu-h-e**) (see Fig. 12, right); the binodal Cooperite (**pts**) with 5 cases and, more surprisingly, the trinodal 4-connected net of Sulvanite (Cu_3VS_4) (**jsa**) with 7 cases. This trinodal network can be described as a **pcu** net decorated by A_3BX_4 cages (see Fig. 13).

3.4. Higher connectivities

Networks with connectivities higher than four are dominated by one topological type, i.e., the 6-connected α-polonium topology (see Table 8) [24]. The majority of the α-Po (**pcu**) nets are 2-fold interpenetrated (12 cases), with few exceptional cases showing $Z = 3$ (5 cases).

Starting from the pcu topology different types of decoration of the nodes have been observed (one example has been described above, i.e., Sulvanite, see

Table 7
Interpenetrating non-diamondoid 4-connected networks [23]

Collection code	Compound (Sp. Gr.)	Nodes[a]	Class	Z	PICVR	Non-Transl	Transl
Gismondine ($4^3.6^2.8$) **gis**							
20033[b]	$Ce(IO_3)_4$ ($P42/n$)	IO_3 4-conn [Ce]	Ia	2	2		[001] (5.32 Å)
lcv ($3^2.10^4$) (*srs-e*)							
58854	Bi_4Rh ($Ia\bar{3}d$)	Rh 4-conn (8-coor)/Bi spacers	IIa	2	1	$\bar{1}$	
lvt ($4^2.8^4$)							
20483	$KC(NO_2)_3$ ($I4_1md$)	K 4-conn $C(NO_2)_3$ 4-conn	IIa	2	1	*d-glide*	
Quartz **qtz**							
408026	$Ag_2Cs(B_{15}O_{24})$ ($P2_12_12$)	B_5O_6/O spacers	Ia	2	2		[001] (5.13 Å)
83675	$Zn[Au(CN)_2]_2$ ($P6_422$)	Zn tet/$Au(CN)_2$ spacers	IIIa	6(3*2)	3	2-axis	[010] (8.45 Å)
41197	$Co[Au(CN)_2]_2$ ($P6_422$)	Co tet/$Au(CN)_2$ spacers	IIIa	6(3*2)	3	2-axis	[010] (8.43 Å)
NbO **nbo**							
400773	$Ba(Nb_3O_6)$ ($R3m$)	Nb/O spacers [Ba]	Ia	2	2		[001] (3.49 Å)
$SrAl_2$, $CeCu_2$ **sra**							
22140[b]	PBr_5 ($Pbcm$)	P tet, Br tet/Br spacers	Ia	2	2		[100] (5.66 Å)
30855	$NaCo(CO)_4$ ($Pbcm$)	Co tet, Na tet/CO spacers	Ia	2	2		[100] (5.53 Å)
$CdSO_4$ **cds**							
65837	$(Se_6I)(SbF_6)$ ($P2/n$)	Se_6 4-conn/I,SbF_6 spacers	Ia	2	2		[010] (7.03 Å)
pcu-h-e *binodal* ($3^2.10^2.11^2$)($3^2.6.7^2.8$)$_2$							
412922	$Mg[B(PO_4)(OH)_2](H_2O)_2$ ($R\bar{3}c$)	Mg oct, B tet, P tet	IIa	2	1	$\bar{1}$	
411449	$(Ni_{0.5}Mg_{0.5})[B(PO_4)(OH)_2](H_2O)_2$ ($R\bar{3}c$)	Mg oct, B tet, P tet	IIa	2	1	**$\bar{1}$**	
PtS, *Cooperite* **pts** *bimodal*							
23467	$PbPbF_6$ ($P\bar{4}c2$)	Pb tet, Pb oct/F spacers	Ia	2	2		[010] (5.20 Å)
25025	$KBiF_6$ ($P\bar{4}c2$)	K tet, Bi oct/F spacers	Ia	2	2		[010] (5.25 Å)
16729	$KNbF_6$ ($P\bar{4}c2$)	K tet, Nb oct/F spacers	Ia	2	2		[010] (5.18 Å)
42509[b]	$KSbF_6$ ($P4_2/mcm$)	K tet, Sb oct/F spacers	Ia	2	2		[010] (5.16 Å)
411796	$AgTaF_6$ ($P4_2/mcm$)	Ag tet, Ta oct/F spacers	Ia	2	2		[010] (4.99 Å)
Cu_3VS_4 *Sulvanite,* **jsa** *trinodal* ($4^2.8^4$)$_3$($4^3.6^3$)$_4$(4^6)							
200270[b]	Tl_3VS_4 ($I\bar{4}3m$)	Tl,V,S	Ia	2	2		[1/2 1/2 1/2] (6.70 Å)
16571[b]	Tl_3TaS_4 ($I\bar{4}3m$)	Tl,Ta,S	Ia	2	2		[1/2 1/2 1/2] (6.64 Å)
52431	Tl_3TaSe_4 ($I\bar{4}3m$)	Tl,Ta,Se	Ia	2	2		[1/2 1/2 1/2] (6.82 Å)
41895[b]	K_3SbS_4 ($I\bar{4}3m$)	K,Sb,S	Ia	2	2		[1/2 1/2 1/2] (6.64 Å)
44707[b]	Na_3SbS_4 ($I\bar{4}3m$)	Na,Sb,S	Ia	2	2		[1/2 1/2 1/2] (6.21 Å)
65141	Na_3SbSe_4 ($I\bar{4}3m$)	Na,Sb,Se	Ia	2	2		[1/2 1/2 1/2] (6.50 Å)
80283	$K_2BaSnTe_4$ ($I\bar{4}3m$)	$K_{2/3}Ba_{1/3}$, Sn, Te	Ia	2	2		[1/2 1/2 1/2] (7.27 Å)

[a]Atoms or groups indicated in [ ] are not considered in the topological analysis.
[b]Multiple entry: different structure determinations with different codes.

Fig. 13). An uncommon type of decoration is present in $Li_9B_{19}S_{33}$ (73151): the nodes are $B_{19}S_{30}$ clusters consisting of two fused T3 supertetrahedra sharing a corner (see Fig. 10, bottom).

By decorating **pcu** nets with octahedra we obtain augmented α-Po nets (**pcu-a** or **cab** from the prototypical CaB_6). Three examples of 2-fold interpenetrated **cab** networks are listed in Table 8, and a schematic view of the interpenetration is shown in Fig. 14. Note that considering as nodes, instead of the whole octahedra, the individual atoms at the octahedral corners we obtain a 5-connected network with Schläfli symbol (**$3^4.4^2.8^4$**). When the decoration consists of centered octahedra (see Fig. 14, right) we obtain a decorated **pcu** net that can be described as **cab** "centered". Seven cases of 2-fold interpenetrating nets with this topology, belonging to Class Ia, are known.

Table 8 contains also a 6-connected network with topology different from **pcu**, observed for the 3-fold interpenetrated $Eu(Ag(CN)_2)_3(H_2O)_3$ (81234), of the type WC (**acs**), that is illustrated in Fig. 15, top left. [25]

3.5. Nodes of different connectivity

A group of 11 interpenetrated nets containing nodes of different connectivities [(3,4), (3,6), and (4,12)] is listed in Table 9 [26]. Among these species it is worth mentioning the 2-fold interpenetrating (3,4)-connected (8^3)$_2$(8^6) net (**tfa**) in $Cs(B_9O_{14})$ (97512) containing 3-connected and 4-connected B_3O_3 nodes (see Fig. 15, top

Table 8
Interpenetrating α-Polonium (**pcu**) and related networks [24]

Collection code	Compound (Sp. Gr.)	Nodes[a]	Class	Z	PICVR	Non-Transl	Transl
α-Po, primitive cubic, **pcu**							
281147	$[Co(H_2O)_4)_3(W_6S_8(CN)_6)(H_2O)_{23.13}$ ($C2/c$)	W_6S_8 6-conn/Co spacers	Ia	2	2		[1/2 1/2 0](13.11 Å)
281146	$Fe(H_2O)_4]_3(W_6S_8(CN)_6)(H_2O)_{24.62}$ ($C2/c$)	W_6S_8 6-conn/Fe spacers	Ia	2	2		[1/2 1/2 0] (13.19 Å)
281145	$[Mn(H_2O)_4)_3(W_6S_8(CN)_6)(H_2O)_{23.4}$ ($C2/c$)	W_6S_8 6-conn/Co spacers	Ia	2	2		[1/2 1/2 0] (13.25 Å)
44692	La_2O_3 ($Im\bar{3}m$)	La oct	Ia	2	2		[1/2 1/2 1/2] (3.91 Å)
100216	Nd_2O_3 ($Im\bar{3}m$)	Nd oct	Ia	2	2		[1/2 1/2 1/2] (3.82 Å)
410239	$[Co(H_2O)_4]_3[V_{18}O_{42}$ $(V_xS_{1-x}O_4)](H_2O)_{24}$ ($Im\bar{3}m$)	$V_{18}O_{42}$ 6-conn/Co spacers	Ia	2	2		[1/2 1/2 1/2] (13.38 Å)
410238	$[Fe(H_2O)_4]_3[V_{18}O_{42}$ $(V_xS_{1-x}O_4)](H_2O)_{24}$ ($Im\bar{3}m$)	$V_{18}O_{42}$ 6-conn/Fe spacers	Ia	2	2		[1/2 1/2 1/2] (13.40 Å)
411144	$(N_2H_5)_2(Mg_3(H_2O)_{12}V_{18}O_{42}(V_xS_{1-x}O_4)) \cdot (H_2O)_{24}$ ($Im\bar{3}m$)	$V_{18}O_{42}$ 6-conn/Mg spacers	Ia	2	2		[1/2 1/2 1/2] (13.42 Å)
411145	$Li_6(Mn_3(H_2O)_{12}V_{18}O_{42}(V_xS_{1-x}O_4)) \cdot (H_2O)_{24}$ ($Im\bar{3}m$)	$V_{18}O_{42}$ 6-conn/Mn spacers	Ia	2	2		[1/2 1/2 1/2] (13.46 Å)
16959[b]	$Co[Ag(CN)_2]_3$ ($P\bar{3}1m$)	Co oct/$Ag(CN)_2$ spacers	Ia	3	3		[010] (7.03 Å)
65699	$K_2Na[Ag(CN)_2]_3$ ($P\bar{3}1m$)	Na oct/$Ag(CN)_2$ spacers, [K]	Ia	3	3		[010] (7.05 Å)
281280	$KMn[Ag(CN)_2]_3$($P312$)	Mn oct/$Ag(CN)_2$ spacers, [K]	Ia	3	3		[010] (6.92 Å)
75503	$RbCd[Ag(CN)_2]_3$($P312$)	Cd oct/$Ag(CN)_2$ spacers, [Rb]	Ia	3	3		[010] (6.92 Å)
201056	$KCo[Au(CN)_2]_3$($P312$)	Co oct/$Au(CN)_2$ spacers, [K]	Ia	3	3		[010] (6.83 Å)
87982	$H_6Mn_3[V_{19}O_{46}(H_2O)_{12}](H_2O)_{30}$ ($Pn\bar{3}$)	$V_{19}O_{46}(H_2O)_{12}$/Mn spacers	IIa	2	1	$\bar{1}$	
73151	$Li_9B_{19}S_{33}$ ($C2/c$)	$B_{19}S_{30}$, fused T3 [Li]	IIa	2	1	$\bar{1}$	
100139[b]	$Fe(OH)Te_2O_5$ ($I4_1$/acd) Mackayite	$Fe_2Te_4O_4$/OH, O spacers	IIa	2	1	$\bar{1}$	
Augmented α-Po, 5-conn ($3^4.4^2.8^4$), **pcu-a cab** (CaB_6 *prototype*)							
25769	Nb_6F_{15} ($Im\bar{3}m$)	Nb_6F_{12}, Nb 5-conn	Ia	2	2		[1/2 1/2 1/2] (7.09 Å)
69053[b]	$Th_6H_7Br_{15}$ ($Im\bar{3}m$)	Th_6Br_{12}, Th 5-conn	Ia	2	2		[1/2 1/2 1/2] (9.93 Å)
69054[b]	$Th_6D_7Br_{15}$ ($Im\bar{3}m$)	Th_6Br_{12}, Th 5-conn	Ia	2	2		[1/2 1/2 1/2] (9.85 Å)
Decorated α-Po, 6-conn ($3^{12}.4^3$)($3^8.4^2.8^4.9$)$_6$, **cab** "**centered**"							
71148	Zr_6CoCl_{15} ($Im\bar{3}m$)	Co centered Zr_6Cl_{12}, Zr 6-conn	Ia	2	2		[1/2 1/2 1/2] (8.82 Å)
71149	Zr_6NiCl_{15} ($Im\bar{3}m$)	Ni centered Zr_6Cl_{12}, Zr 6-conn	Ia	2	2		[1/2 1/2 1/2] (8.83 Å)
33926	$CoTh_6Br_{15}$ ($Im\bar{3}m$)	Co centered Th_6Br_{12}, Th 6-conn	Ia	2	2		[1/2 1/2 1/2] (9.97 Å)
33925	$FeTh_6Br_{15}$ ($Im\bar{3}m$)	Fe centered Th_6Br_{12}, Th 6-conn	Ia	2	2		[1/2 1/2 1/2] (9.95 Å)
33927	$NaFeTh_6Br_{15}$ ($Im\bar{3}m$)	Fe centered Th_6Br_{12}, Th 6-conn [Na]	Ia	2	2		[1/2 1/2 1/2] (10.05 Å)
71146	$Li_2Zr_6MnCl_{15}$ ($Im\bar{3}m$)	Mn centered Zr_6Cl_{12}, Zr 6-conn [Li]	Ia	2	2		[1/2 1/2 1/2] (8.89 Å)
71147	$Li_2Zr_6FeCl_{15}$ ($Im\bar{3}m$)	Fe centered Zr_6Cl_{12}, Zr 6-conn [Li]	Ia	2	2		[1/2 1/2 1/2] (8.89 Å)
WC 6-*conn* ($4^9.6^6$), **acs**							
81234	$Eu(Ag(CN)_2)_3(H_2O)_3$ ($P6_3/mcm$)	Eu 9-coor/$Ag(CN)_2$ spacers	Ia	3	3		[010] (6.69 Å)

[a]Atoms or groups indicated in [ ] are not considered in the topological analysis.
[b]Multiple entry: different structure determinations with different codes.

Table 9
Interpenetrating networks with nodes of different connectivities [26]

Collection code	Compound (Sp. Gr.)	Nodes[a]	Class	Z	PICVR	Non-Transl	Transl
3,4-*conn* $(8^3)_2(8^6)$-*Wells uniform* $(8^3)(8^6)$-*b*, **tfa**							
99793[b]	$Cs(B_9O_{14})$ ($P222_1$)	B_3O_3 3-conn, B_3O_3 4-conn	IIa	2	1	2-axis	
3,4-*conn* $(4.8^2)(4.8^5)$ **dmc**[c]							
201713	Ag_2HgS_2 ($P2_1/c$) Imiterite	Ag 3-conn, S 4-conn	Ia	2	2		[100] (4.04 Å)
3,4-*conn tetranodal* $(4^2.6)(6^3)(4^2.6^3.8)$ $(6^5.8)$							
412298	$Hg_2[B(CN)_4]_2$ (*Pbcm*)	Hg 4-conn, B 3-conn	Ia	2	2		[100] (5.69 Å)
3,4-*conn pentanodal* $(4.8^2)(4.8^5)$ VS $= [4.8_4.8_3.8_3.8_3.8_3](c_{10} = 785)[4.8_4.8_3.8_3.8_3.8_3]_2(c_{10} = 777)[4.8_2.8_2](c_{10} = 763,759,771]$							
89686[b]	Hg_3OCl ($C2/c$) Poyarkovite	O 4-conn, Hg 3-conn [Cl]	Ia	2	2		[1/21/20] (10.52 Å)
3,6-*conn* $(4^3)_2(4^6.12^9)$ PrI_2 **spn**							
404375	$Cu_2(Mo_6Cl_{14})$ ($Pn\bar{3}$)	Cu 3-conn, Mo_6Cl_{14} 6-conn	Ia	2	2		[100] (12.77 Å)
409272	$Cu_2(W_6Cl_{14})$ ($Pn\bar{3}$)	Cu 3-conn, W_6Cl_{14} 6-conn	Ia	2	2		[100] (12.81 Å)
404376	$Cu_2(Mo_6Br_{14})$ ($Pn\bar{3}$)	Cu 3-conn, Mo_6Br_{14} 6-conn	Ia	2	2		[100] (13.35 Å)
83581[b]	$Cu_2(W_6Br_{14})$ ($Pn\bar{3}$)	Cu 3-conn, W_6Br_{14} 6-conn	Ia	2	2		[100] (13.39 Å)
γ-MnO_2 *Ramsdellite*, 3,6-*conn trinodal* $(4.6^2)(4^3)(4^4.6^8.8^3)$							
86652	$[Zn(H_2O)]_2\{S_8[Re(CN)]_6\}(H_2O)_7$ (*Pbcn*)	S_8Re_6 6-conn, $Zn(CN)_3(H_2O)$ 3-conn	IIa	2	1	$\bar{1}$	
4,12-*conn* $(4^{36}.6^{30})(4^4.6^2)_3$ Cu_3Au **ftw**							
32054	$Pd_{13}Cu_3S_7$ ($I\bar{4}3m$)	S_4Pd_3Cu 12-conn S 4-conn/Pd spacers; Pd-Pd neglected	Ia	2	2		[1/2 1/2 1/2] (7.69 Å)
77887[b]	$Pd_{16}S_7$ ($I\bar{4}3m$) Vasilite	S_4Pd_4 12-conn S 4-conn/Pd spacers; Pd-Pd neglected	Ia	2	2		[1/2 1/2 1/2] (7.73 Å)

[a]Atoms or groups indicated in [ ] are not considered in the topological analysis.
[b]Multiple entry: different structure determinations with different codes.
[c]Observed also in a Metal-Organic network in CSD (Refcode XAYYUR).

Table 10
Non-equivalent and hetero-interpenetrating networks [28]

Collection code	Compound (Sp. Gr.)	Nodes[a]	Z
Non-equivalent interpenetrating nets			
$SrSi_2$ *uniform* (10^3)-*a* **srs**			
201659	Ta_4PS_{29} ($P4_32_12$)	Ta oct/PS_4, S_2 spacers + 1D S-chain	2(1 + 1) + 1D
$ThSi_2$ *uniform* (10^3)-*b* **ths**			
71358[b]	$LiNa_2K(Fe_{1.63}Mg_{0.37})(Si_4O_{12})_2$(Cc) Neptunite	SiO_4 3-conn, [Li,Na,K,Fe,Mg]	2(1 + 1)
Diamond **dia**			
71947	$K_4[Pd(Se_4)_2][Pd(Se_6)_2]$ ($I2_12_12_1$)	$PdSe_8$, $PdSe_{12}$, [K]	2(1 + 1)
α-Po **pcu**			
412499	$Hg_3CdCl_2(SCN)_6$ ($R3c$)	Cd oct/$Hg(SCN)_2$ spacers, [Cl]	2(1 + 1)
Hetero-interpenetrating nets			
dia + 6-conn **crs** (**dia-e**) ($3^6.6^6.7^3$)			
Pyrochlore related	$A_2B_2X_6X'$ X = F,O,OH X' = F, S, O,OH,H_2O	$X'A_2$ (dia) A spacer//BX_3(crs) B oct. approx 600 compounds almost all in $Fd\bar{3}m$	2(1 + 1)
srs + 6-*conn* **lcy** ($3^3.5^9.6^3$)			
84931	Li_2Pt_3B ($P4_332$)	Li (srs)//B oct Pt spacer (lcy)	2(1 + 1)
dia 2fold + **nbo**			
10172	$Bi_3GaSb_2O_{11}$ ($Pn\bar{3}$)	Bi_4O_4/Bi spacer (dia)//Sb_2O_6 (nbo) Sb/Ga .67/.33	3(2 + 1)
82633[b]	$Bi_3AlSb_2O_{11}$ ($Pn\bar{3}$)	Bi_4O_4/Bi spacer (dia)//Sb_2O_6 (nbo) Sb/Al .67/.33	3(2 + 1)
100517	$La_3Ru_3O_{11}$ ($Pn\bar{3}$)	La_4O_4/La spacer (dia)//Ru_2O_6 (nbo)	3(2 + 1)
200472	$La_3Ir_3O_{11}$ ($Pn\bar{3}$)	La_4O_4/La spacer (dia)//Ir_2O_6 (nbo)	3(2 + 1)
24955[b]	$Bi_3Ru_3O_{11}$ ($Pn\bar{3}$)	Bi_4O_4/Bi spacer (dia)//Ru_2O_6 (nbo)	3(2 + 1)
79859	$NaBi_2Sb_3O_{11}$ ($Pn\bar{3}$)	Bi_4O_4/Na spacer (dia)//Sb_2O_6 (nbo)	3(2 + 1)
dia 2fold + *Sodalite* **sod**			
67819	$[Ho_2(Pb_4O_4)](Al_6O_{12})$ ($Pn\bar{3}m$)	Pb_4O_4/Ho (dia)//Al tet (sod)	3(2 + 1)
67820	$[Lu_2(Pb_4O_4)](Al_6O_{12})$ ($Pn\bar{3}m$)	Pb_4O_4/Lu (dia)//Al tet (sod)	3(2 + 1)
404478	$[Eu_2(Pb_4O_4)](Al_6O_{12})$ ($Pn\bar{3}m$)	Pb_4O_4/Eu (dia)//Al tet (sod)	3(2 + 1)
404479	$[Gd_2(Pb_4O_4)](Al_6O_{12})$ ($Pn\bar{3}m$)	Pb_4O_4/Gd (dia)//Al tet (sod)	3(2 + 1)
406531	$[Nd_2(Pb_4O_4)](Al_6O_{12})$ ($Pn\bar{3}m$)	Pb_4O_4/Nd (dia)//Al tet (sod)	3(2 + 1)
406532	$[Sm_2(Pb_4O_4)](Al_6O_{12})$ ($Pn\bar{3}m$)	Pb_4O_4/Sm (dia)//Al tet (sod)	3(2 + 1)

[a]Atoms or groups indicated in [ ] are not considered in the topological analysis.
[b]Multiple entry: different structure determinations with different codes.

right). This is the Wells uniform (8^3)(8^6)-b network [4c]. The (3,4)-connected **dmc** net was previously found by us in CSD as refcode XAYYUR with the same kind of interpenetration (2-fold Class Ia) (see Fig. 15, center left). A net derived from packing of cubes observed in PrI_2 (**spn**) is observed in four species where the 6 connected nodes are M_6X_{12} octahedra (see Fig. 15, center right). The topology of Ramsdellite (γ-MnO_2) [27], a trinodal (3,6)-connected net, is observed in $[Zn(H_2O)]_2\{S_8[Re(CN)]_6\}(H_2O)_7$ (866529) with the 6-conn centers decorated with face-capped octahedra $[S_8Re_6]$. Of interest are also two examples, $Pd_{13}Cu_3S_7$ (32054) and $Pd_{16}S_7$ (77887), that show (4,12)-connected nets (2-fold interpenetrated) with the Cu_3Au (**ftw**) topology, illustrated in Fig. 15, bottom left.

3.6. Non-equivalent and hetero-interpenetrating nets

These are entangled 3D nets that are not related by translations or symmetry operations. When the nets are of the same kind we are in the case of "non-equivalent" interpenetration (already observed in CSD [1] for few cases); if the nets are different we have the new case of "hetero-interpenetration". The Z values are described in terms of the sum of groups of equivalent nets. Inorganic interpenetrating networks of this family can differ for topology or composition, but also simply for small structural variations of the same architecture. These species are reported in Table 10 [28]. The list shows few structural types but some of these include many examples, as, in particular, the pyrochlore structure.

Compound Ta_4PS_{29} (201659) has been placed here because it contains two homochiral $SrSi_2$ (**srs**) non-equivalent nets that are threaded by 1D helical sulphur chains. Thus we can say that this interpenetration is of the type 2(1 + 1) + 1D.

In $LiNa_2K(Fe_{1.63}Mg_{0.37})(Si_4O_{12})_2$ (Neptunite) the two interpenetrating $ThSi_2$ (**ths**) nets are not symmetry equivalent. The same non-equivalence is observed for the two interpenetrating **pcu** nets of $Hg_3CdCl_2(SCN)_6$

Table 11
Interpenetrating H-bonded 3D networks [29]

Collection code	Compound (Sp. Gr.)	Nodes[a]	Class	Z	PICVR	Non-Transl	Transl
$SrSi_2$ **srs**							
66552	$(H_3O)(SbF_6)$ ($I2_13$)	O, SbF_6 3-conn {O–H–F}	Ia	2	2		[1/21/21/2](8.76 Å)
40446	NH_2CN (*Pbca*)[b]	both N atoms {N–H–N}	IIa	2	1	$\bar{1}$	
23835	$[C(NH_2)_3]Cl$ (*Pbca*)	$C(NH_2)_3$, Cl 3-conn, {N–H–Cl}	IIa	2	1	$\bar{1}$	
$ThSi_2$ **ths**							
9653	$H_2Te_2O_3F_4$ (*Fdd2*)	Te {O–H–F}	Ia	3	3		[001] (4.76 Å)
281646[c]	$\{Cu[(NH_2)_2CS]_3\}Cl$ ($P4_32_12$)	Cu, S {N–H–Cl}	IIa	2	1	2-*axis*	
281647	$\{Cu[(NH_2)_2CS]_3\}Br$ ($P4_12_12$)	Cu, S {N–H–Br}	IIa	2	1	2-*axis*	
Diamond **dia**							
43300	NH_4Br I ($P\bar{4}3m$)	Br tet, N tet {Br–H–N}	Ia	2	2		[010] (4.06 Å)
22154	NH_4I III ($P\bar{4}3m$)[d]	I tet, N tet {I–H–N}	Ia	2	2		[010] (4.32 Å)
31868	H_2O Ice VII ($Pn\bar{3}m$)	Cu_2O type	Ia	2	2		[010] (3.30 Å)
64773[c]	D_2O Ice VII ($Pn\bar{3}m$)	Cu_2O type	Ia	2	2		[010] (3.35 Å)
44102[c]	D_2O Ice VIII ($I4_1/amd$)	Cu_2O type	IIa	2	1	$\bar{1}$	
67267	$(D_2O)_2(DF)_3$ ($R\bar{3}c$)	F, O {O–D–F}	IIa	2	1	$\bar{1}$	
280083[c]	$(NH_4)(IO_4)$ ($I4_1/a$)	I tet, N tet {O–H–N}	IIa	2	1	$\bar{1}$	
23280	$(ND_4)(IO_4)$ ($I4_1/a$)	I tet, N tet {O–H–N}	IIa	2	1	$\bar{1}$	
1394[c]	$(NH_4)(ReO_4)$ ($I4_1/a$)	Re tet, N tet {O–H–N}	IIa	2	1	$\bar{1}$	
77923[c]	$(ND_4)(ReO_4)$ ($I4_1/a$)	Re tet, N tet {O–H–N}	IIa	2	1	$\bar{1}$	
38337	$NH_4[F(HF)_3]$ *R*3*c*	$[F(HF)_3]$ tet, N tet {F–H–N}	IIa	2	1	*c-glide*	
($4^2.8^4$) **lvt**							
92579	$CdCl_2[(NH_2)_2CS]_4$ ($P4_2/n$)	whole molecule {N–H–Cl}	Ia	2	2		[001] (9.27 Å)
50333	H_2S IV h.p. ($I4_1/acd$)	S {S–H–S}	IIa	2	1	$\bar{1}$	
$CdSO_4$ **cds**							
413139	$Rb(H_2C_6N_9)(H_2O)_{0.5}$	$(H_2C_6N_9)$ dimers {N–H–N}, {O–H–N} [Rb]	Ia	3	3		[010] (5.12 Å)
$SrAl_2$ $CeCu_2$ **sra**							
413097	$(NH_4)[N(CN)_2]$ ($P2_1/c$)	NH_4 tet, $N(CN)_2$ 4-conn {N–H–N}	Ia	2	2		[100] (3.79 Å)
281696[c]	$(ND_4)[N(CN)_2]$ ($P2_1/c$)	ND_4 tet,$N(CN)_2$ 4-conn {N–D–N}	Ia	2	2		[100] (3.79 Å)
Not reported	$(NH_4)[N(NO_2)_2]$ ($P2_1/c$)	NH_4 tet, $N(NO_2)_2$ 4-conn {N–H–O}	Ia	2	2		[100] (6.91 Å)
15353	$HCl(H_2O)_2$ ($P2_1/c$)	H_5O_2, Cl, 4-conn {O–H–Cl}	Ia	2	2		[100] (3.99 Å)
34105	$HBr(H_2O)_2$ ($P2_1/c$)	H_5O_2, Br, 4-conn {O–H–Brl}	Ia	2	2		[100] (4.23 Å)
Zeolite edingtonite $(4^2.8^4)(4^3.8^3)_4$ **edi**							
16950	H_2O Ice VI ($P4_2/nmc$)	O tet	IIa	2	1	$\bar{1}$	
201702	D_2O Ice VI ($P4_2/nmc$)	O tet	IIa	2	1	$\bar{1}$	
PtS, *Cooperite* **pts** *bimodal*							
14140[c]	NH_4HF_2 (*Pman*)	N tet, HF_2 {F–H–N}	Ia	2	2		[001] (3.67 Å)
412211[c]	NH_4N_3 (*Pmna*)	N tet, N_3 {N–H–N}	Ia	2	2		[010] (3.78 Å)
37128	$(NH_4)(NO_3)$ (*Pccn*)	N tet, NO_3 {O–H–N}	IIa	2	1	2-*axis*	
35435[c]	$(ND_4)(NO_3)$ (*Pccn*)	N tet, NO_3 {O–D–N}	IIa	2	1	2-*axis*	
α-*Po primitive cubic* **pcu**							
67575[c]	$(NH_4)_6(MnMo_9O_{32})(H_2O)_6$ (*R*32)[d]	$MnMo_9O_{32}$ 6-conn/NH_4 spacers {O–H–N}	Ia	2	2		[001] (12.42 Å)
49909[c]	$(NH_4)_6(NiMo_9O_{32})(H_2O)_6$ (*R*32)[d]	$NiMo_9O_{32}$ 6-conn/NH_4 spacers {O–H–N}	Ia	2	2		[001] (12.41 Å)
31274	$LiNa_2H[Al(PO_4)_2(OH)]$ (*Pbcb*) tancoite	Al oct {O–H–O} [Li,Na]	Ia	2	2		[100] (6.95 Å)
2862[c]	$H_3Co(CN)_6$ ($P\bar{3}1m$)	Co oct {N–H–N}	Ia	3	3		[001] (5.70 Å)
9484[c]	$D_3Co(CN)_6$ ($P\bar{3}1m$)	Co oct {N–D–N}	Ia	3	3		[001] (5.72 Å)
2861	$H_3Fe(CN)_6$ ($P\bar{3}1m$)	Fe oct {N–H–N}	Ia	3	3		[001] (5.78 Å)

[a]In {A–H–B} the type of hydrogen bond; atoms indicated in [ ] are not considered in the topological analysis.
[b]Observed also in CSD (Refcode CYANAM01).
[c]Multiple entry: different structure determinations with different codes.
[d]Hydrogen atom positions are generated by Topos.

(412499). On the other hand, $K_4[Pd(Se_4)_2][Pd(Se_6)_2]$ (71947) is remarkable because it contains two **dia** networks of different composition.

Hetero-interpenetration is dominated by the very large family of compounds with the pyrochlore structure. According to classic description they have the common formula $A_2B_2X_6X'$ (X = F, Cl, O, OH; X' = F, O, OH, H_2O, S)[4a]. In ICSD there are approximately 600 Collection codes related to this structure type, that may be described as comprised of two mutually

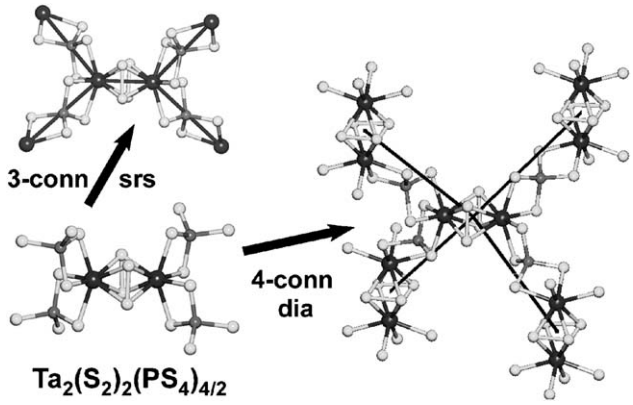

Fig. 2. A different selection of nodes in $Ta(PS_4)S_2$ (23284) can lead to the 3-connected **srs** net or to the 4-connected **dia** net.

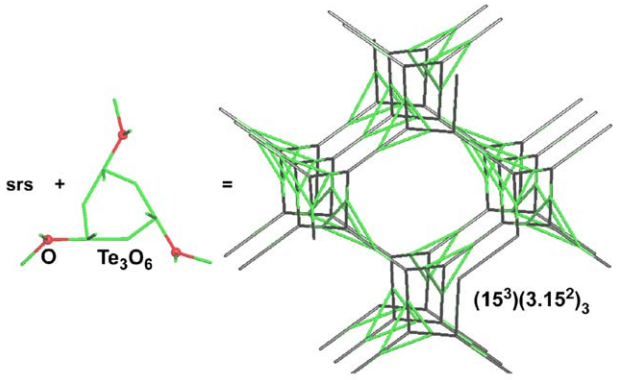

Fig. 3. The hemi-decorated **srs** net in $K(GaTe_6O_{14})$ (280793), with alternating 3-connected O and 3-connected Te_3O_6 triangles as nodes.

interpenetrated nets: one ($X'A_2$ nodes) with the **dia** topology and the second (BX_3 nodes) 6-connected with the **dia-e** topology (see Fig. 16). The latter net is the 'edge net' derived from diamond and is also called **crs** (from the 'coordination' of the oxygen atoms in cristobalite) (see also Fig. 11 for another case of 'edge net').

In Li_2Pt_3B (84931) the Pt_3B part forms a single rare 4-connected **lcy** net with B nodes and Pt spacers, while the Li atoms give and interpenetrating **srs** net (see Fig. 17).

The family of general formula $A_3B_3O_{11}$ (Sp.Gr. $Pn\bar{3}$, 6 cases) shows a very interesting interpenetrated network topology. An example is $La_3Ru_3O_{11}$ (100517) (see Table 10 and Fig. 18). This structure is comprised of three interpenetrating nets, i.e., two equivalent **dia** nets and one **nbo** net [thus $Z = 3(2 + 1)$]. The two **dia** nets alone form an interpenetrated system generated by translation (Class Ia). As shown in Fig. 18 the nodes of the **dia** networks are La_4O_4 cubane-like units (decorated diamond) while the nodes of the **nbo** net are Ru_2O_6 dimetal groups (decorated NbO).

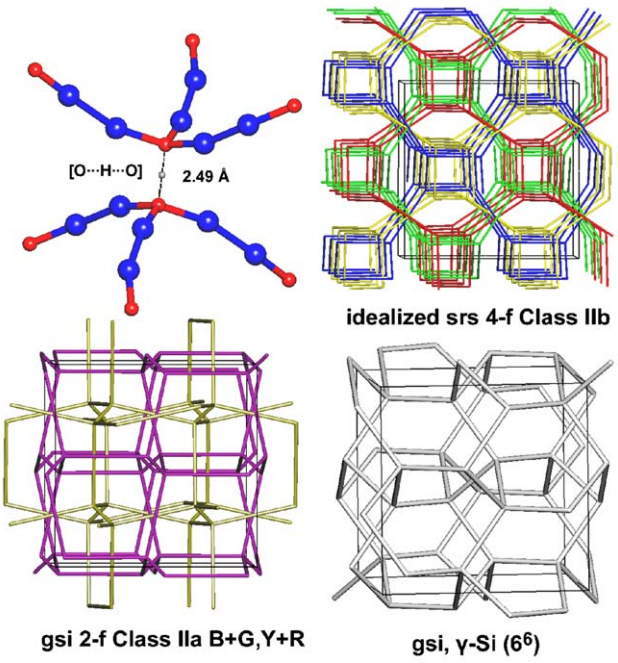

Fig. 4. Eglestonite: (top left) the 3-connected building block $(Hg_2)_3(O/OH)$ showing the H-bond to give a 4-connected node; (top right) the idealized 4-fold **srs** net obtained considering the oxygen valence connectivity only [B (blue)/Y (yellow) and G (green)/R (red) nets related by a 2-fold axis; B/G related to Y/R by a inversion center; (bottom left) the simplified 2-fold 4-connected **gsi** net obtained considering the H-bonds; (bottom right) a single idealized **gsi** net.

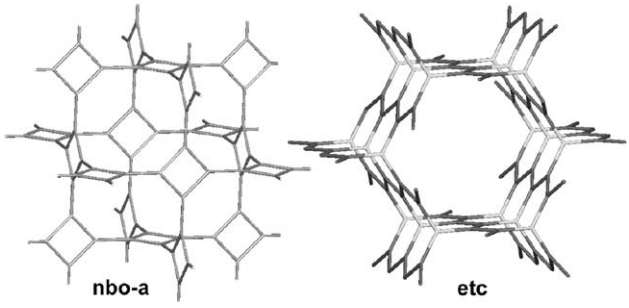

Fig. 5. Two rare 3-connected nets: (left) augmented NbO net (4.12^2) (**nbo-a**) and (right) the binodal uniform (8^3) (**etc**).

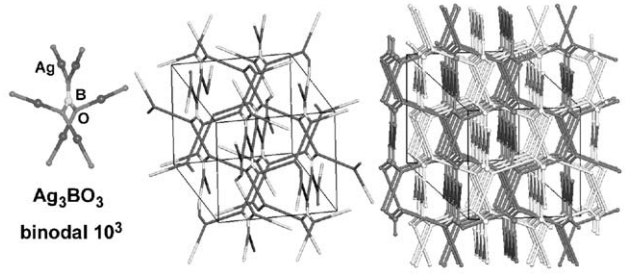

Fig. 6. The new binodal 3-connected uniform (10^3) net observed in β-Ag_3BO_3 (32721): the nodes (left), a single net (middle) and the 2-fold interpenetrated array (right).

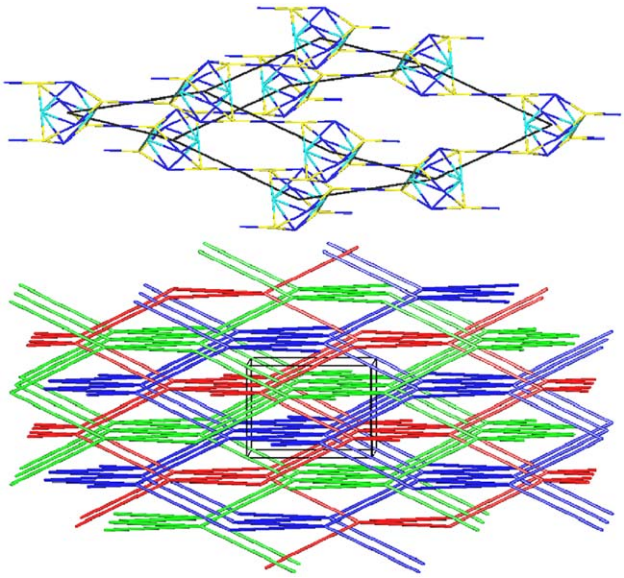

Fig. 7. A single adamantane cage decorated with $Ag_4Cu_2S_4$ clusters in Ag_3CuS_2 (67526) and the ''non-normal'' 3-fold **dia** net (three translationally equivalent nets, Class Ia).

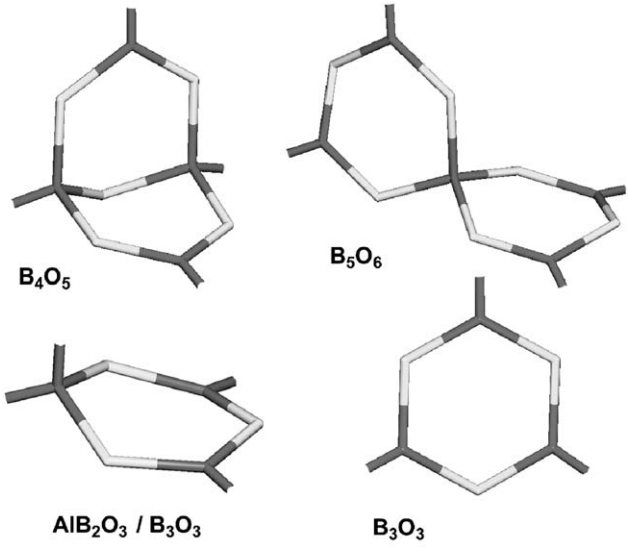

Fig. 8. Observed borates decorating units.

Another interesting group of structures of composition $[Ln_2(Pb_4O_4)](Al_6O_{12})$ consists of three interpenetrating nets, i.e., two equivalent **dia** nets and one sodalite (**sod**) net $[Z = 3(2 + 1)]$, illustrated in Fig. 19. The **dia** nets are decorated by Pb_4O_4 clusters joined by the Ln spacers and the sodalite net has Al tetrahedral nodes. We should mention here, that other cases of heterointerpenetration **dia** + **sod** may be found depending on the choice of the *representation level* (bonding distances *vs* connectivity).

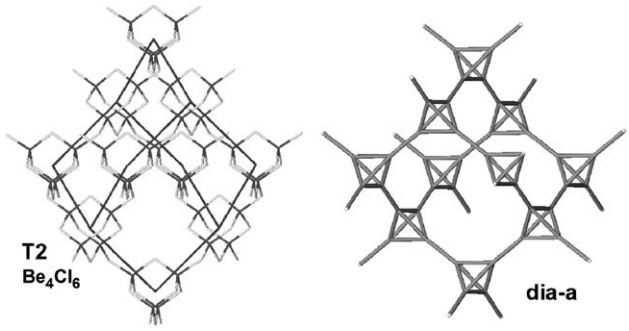

Fig. 9. The prototypical net of $BeCl_2$: a T2-Be_4Cl_6 adamantane cage decorates the diamond net giving a topology classified as **dia-a**, the augmented diamond (decoration with tetrahedra).

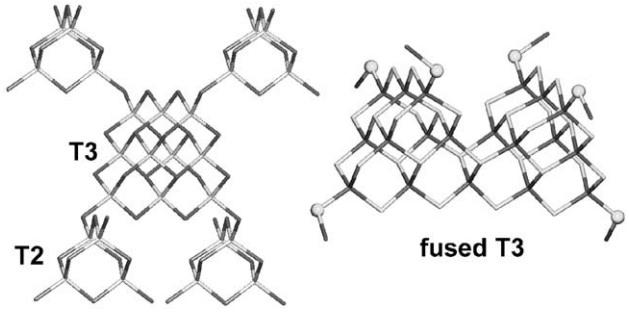

Fig. 10. Different decorations of **dia** with both T2 and T3 (left) and **pcu** with fused T3 (right). White balls indicate the bridging S atoms.

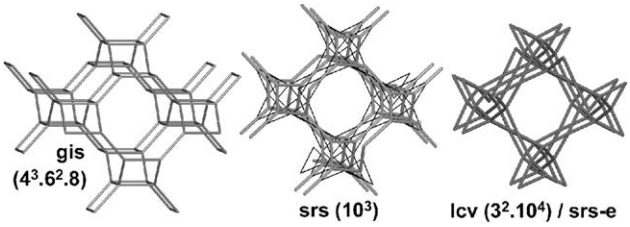

Fig. 11. Rare 4-connected nets: (left) the Gismondine net (**gis**) and the edge net from **srs** (shown in the middle) called (**srs-e**) or also **lcv** (right). An **edge net** (also expanded net) is obtained from the original net by placing vertices in the middle of the edges, discarding the original vertices and edges, and joining the new vertices to enclose the coordination figure of the original vertices (as shown in thin lines superimposed on the **srs** net in the middle).

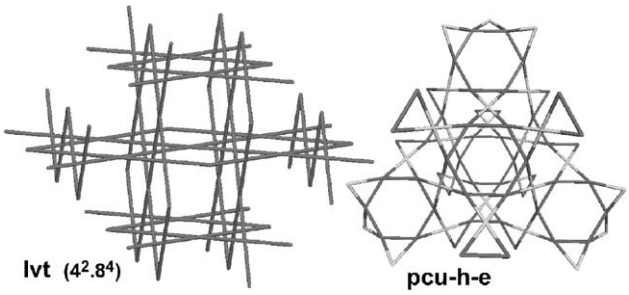

Fig. 12. Rare 4-connected nets: (left) square planar **lvt** and (right) ninodal **pcu-h-e**.

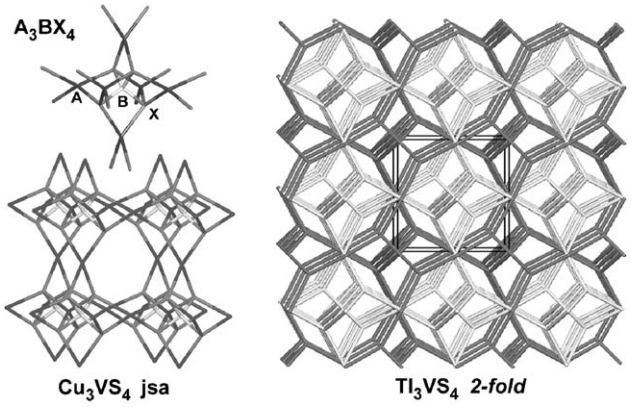

Fig. 13. The **jsa** Sulvanite trinodal 4-connected net as decoration of **pcu** by A_3BX_4 cages.

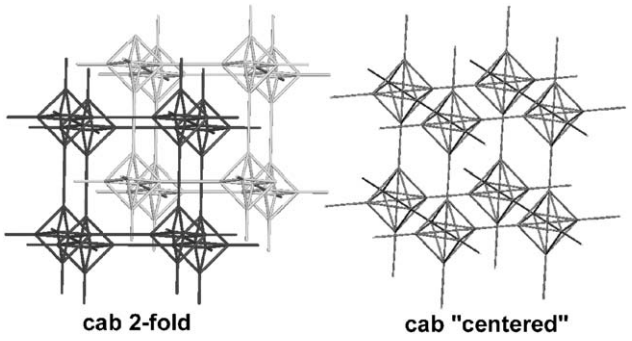

Fig. 14. The **cab** 2-fold interpenetrated net and the **cab "centered"** net.

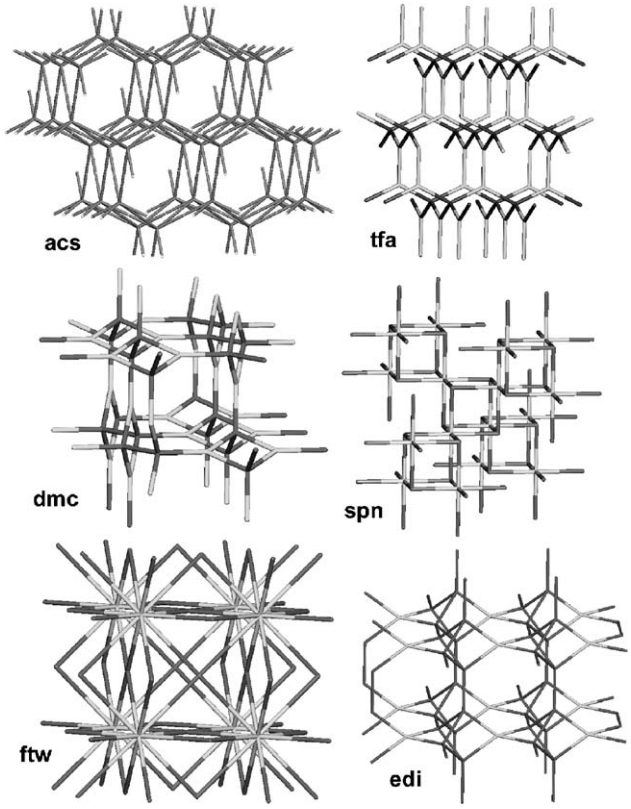

Fig. 15. The 6-conn **acs** net observed in WC (top left) and some binodal rare nets (**tfa**, **dmc**, **spn**, **ftw**, **edi**).

3.7. *Hydrogen bonded interpenetrating 3D networks*

The analysis of H-bonds effects on interpenetration has also been investigated. An example illustrating the impact on topology of the inclusion of H-bonds in addition to valence bonds in the rationalization of 3D interpenetrating nets has been illustrated above for Eglestonite (see Fig. 4). A list of 37 interpenetrating H-bonded 3D networks is given in Table 11 [29]; different topologies are observed, mainly diamond (**dia**), with 11 cases, followed by α-Po (**pcu**), with 6 cases. Our investigation of these nets is based on the geometrical *criteria* previously illustrated, without any detailed analysis of the H-bond synthons [30].

Though, generally speaking, H-bonds, considered in addition to valence bonds, could produce 3D networks by joining 0D (i.e., finite), 1D or 2D motifs, all the examples but two in Table 11 are based on 0D species. The two exceptions are $\{Cu[(NH_2)_2CS]_3\}Cl$ (281646) and $\{Cu[(NH_2)_2CS]_3\}Br$ (281647), in which the $Cu[(NH_2)_2CS]_3$ moieties form 1D helical chains all running in the same direction that are interlinked via H-bond bridges involving the halides. This generates two interpenetrated **ths** nets (see Fig. 20).

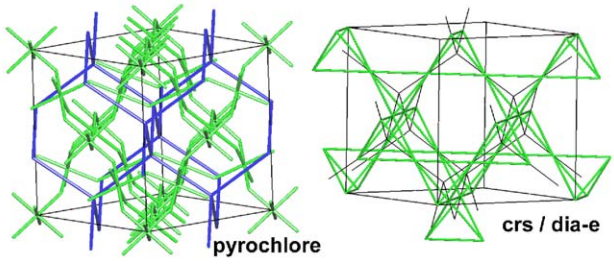

Fig. 16. The pyrochlore structure showing two hetero-interpenetrating nets, with the 4-connected **dia** and 6-connected **dia-e** or **crs** topologies (left); the latter net is the 'edge net' from diamond (right) (see also Fig. 11).

The same topology (**ths**) can be assigned to the 3-fold interpenetrated $H_2Te_2O_3F_4$ (9653), that contains di-nuclear molecules $(HO)F_2TeOTeF_2(OH)$, illustrated in Fig. 21, if we take as nodes the Te atoms. Considering, on the other hand, the whole molecule as a 4-connected node a 3-fold **dia** architecture is obtained (for a similar case see Fig. 2).

An uncommon type of H-bond with bifurcated acceptor [30] is observed in the 2-fold interpenetrated **srs** NH_2CN (40446) (again if the whole molecule is considered as a 4-connected node a 2-fold **dia**

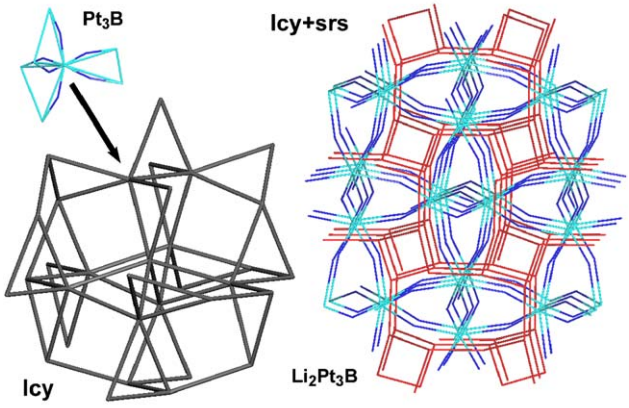

Fig. 17. The hetero-interpenetrating nets **lcy** + **srs** observed in Li2Pt3B (84931) showing the distorted octahedral coordination of the boron atom.

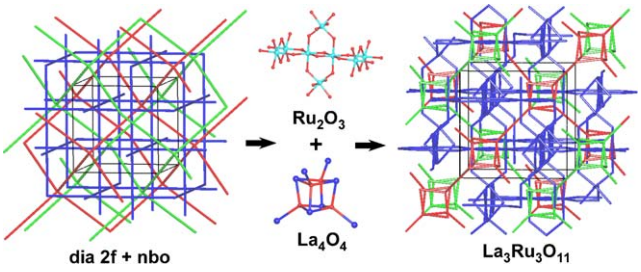

Fig. 18. The three schematized hetero-interpenetrating nets (2-fold **dia** + **nbo**) in the $A_3B_3O_{11}$ family (left): decoration of the nodes with the moieties shown in the middle leads to the network of $La_3Ru_3O_{11}$ (100517) (right).

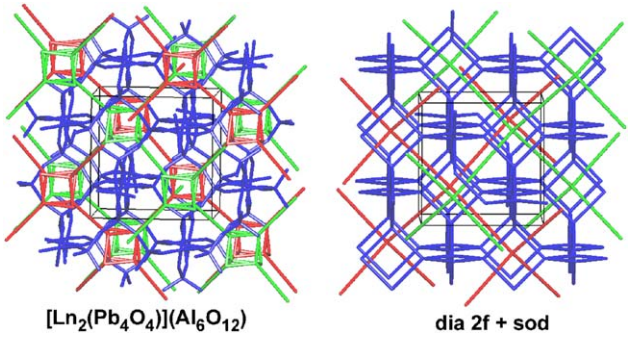

Fig. 19. The hetero-interpenetrating 2-fold **dia** nets and sodalite (**sod**) net in the $[Ln_2(Pb_4O_4)](Al_6O_{12})$ species (left) and the idealized version (right).

architecture is obtained) and in the 2-fold interpenetrated **sra** $(NH_4)[N(CN)_2]$ (413097) (see Fig. 22).

We have examined the interpenetrated networks of Ice VI, VII and VIII. Ice VI (16950) and the D_2O analog (201702) have 2-fold interpenetrated nets related to the Zeolite edingtonite (**edi**), Schläfli symbol $(4^2.8^4)(4^3.8^3)_4$ (see Fig. 15 bottom right). Ice VII and VIII are similar,

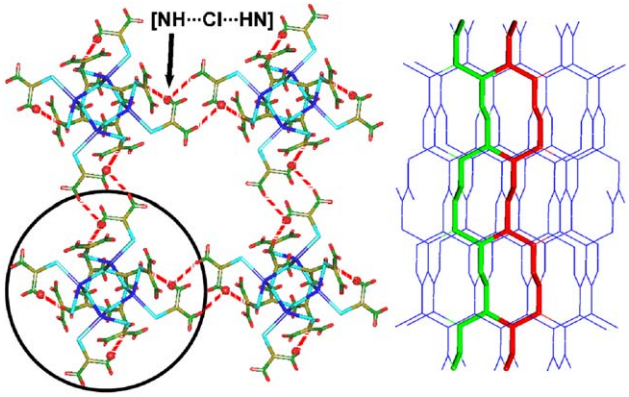

Fig. 20. A single network of the 2-fold interpenetrated **ths** in $\{Cu[(NH_2)_2CS]_3\}Cl$ (281646) and $\{Cu[(NH_2)_2CS]_3\}Br$ (281647), formed via NH···halogen···HN bridges joining parallel 1D helical chains (left, the view is down the chain propagation direction and one chain is evidenced). The location of the chains relative to the **ths** net is also illustrated (right), two of them being evidenced in green and red.

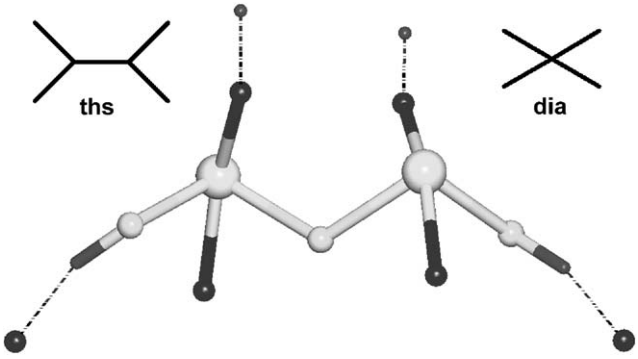

Fig. 21. The different selection of nodes in $H_2Te_2O_3F_4$ (9653).

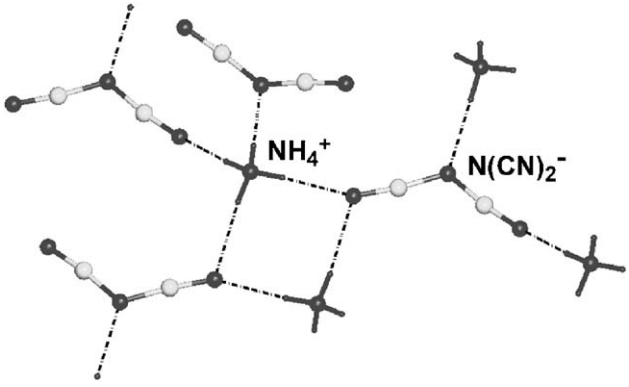

Fig. 22. The H-bonds in the 2-fold interpenetrated **sra** net of $(NH_4)[N(CN)_2]$ (413097).

both with 2-fold **dia** nets, but our analysis reveals that they belong to two different Classes (Ia and IIa, respectively). It is worth noting that this difference could affect some physical properties of the substances caused by translational symmetry (e.g., phonon spectra).

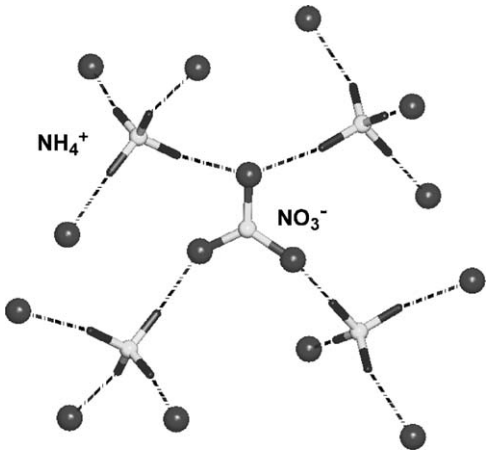

Fig. 23. The H-bonds in the 2-fold interpenetrated cooperite (**pts**) net found in $(NH_4)(NO_3)$ (37128).

A 2-fold interpenetrated network with the cooperite topology (**pts**) is found for $(NH_4)(NO_3)$ (37128) (see Fig. 23).

The α-Po family contains interesting examples: the decametal clusters MMo_9O_{32} [$M = Mn$ (67575), Ni (49909)] are linked via NH_4^+ spacers into 2-fold interpenetrated **pcu** nets. Moreover, hexacyanide complexes like $Co(CN)_6^{3-}$ in compound $H_3Co(CN)_6$ (2862) give interesting 3-fold interpenetrated **pcu** arrays via CN–H–NC bridges.

4. Conclusions

We have discussed above the results of our investigations with TOPOS of interpenetrating 3D inorganic networks in ICSD, sustained both by valence and H-bond interactions. Comprehensive lists of Collection codes have been obtained, that have been organized accordingly to the different node connectivity and net topology (Tables 4–11). Compared with MOFs these inorganic nets show a limited degree of interpenetration (almost all have $Z = 2$); consequently classes are also limited to Ia or IIa (but note that the first example of Class IIb has been established within these species). The choice of the nodes in the ICSD networks was proven to be more difficult and arbitrary than in the previously investigated CSD cases. Alternative views of the nets were frequently found, resulting in motifs of different topology, and adopting a different *level of representation* can even transform an interpenetrated array into a non-interpenetrated one and vice versa.

The results confirm that TOPOS is a powerful tool for the analysis of network interpenetration and that its use can also fruitfully allow finding alternative and less usual rationalizations of inorganic materials.

Acknowledgments

I.A.B. and V.A.B. appreciate the financial support (Grant No. 04-07-90050) of the Russian Foundation for Basic Research. L.C., G.C. and D.M.P. thanks MURST for financing the PRIN 2004-2005.

References

[1] Part I: V.A. Blatov, L. Carlucci, G. Ciani, D.M. Proserpio, CrystEngComm. 6 (2004) 377–395.
[2] (a) N.W. Ockwig, O. Delgado Friedrichs, M. O'Keeffe, O.M. Yaghi, Acc. Chem. Res. 38 (2005) 176–182;
(b) S. Kitagawa, R. Kitaura, S. Noro, Angew. Chem. Int. Ed. 43 (2004) 2334–2375;
(c) O.M. Yaghi, M. O'Keeffe, M. Eddaoudi, H.K. Chae, J. Kim, N.W. Ockwig, Nature (London) 423 (2003) 705–714;
(d) C. Janiak, Dalton Trans. (2003) 2781–2804;
(e) S.L. James, Chem. Soc. Rev. 32 (2003) 276–288;
(f) B. Moulton, M.J. Zaworotko, Chem. Rev. 101 (2001) 1629–1658;
(g) A.K. Cheetham, G. Ferey, T. Loiseau, Angew. Chem. Int. Ed. 38 (1999) 3269–3292;
(h) A.J. Blake, N.R. Champness, P. Hubberstey, W.S. Li, M.A. Withersby, M. Schröder, Coord. Chem. Rev. 183 (1999) 117–138;
(i) A.N. Khlobystov, A.J. Blake, N.R. Champness, D.A. Lemenovskii, A.G. Majouga, N.V. Zyk, M. Schröder, Coord. Chem. Rev. 222 (2001) 155–192.
[3] (a) S.R. Batten, R. Robson, Angew. Chem. Int. Ed. Engl. 37 (1998) 1460–1494;
(b) L. Carlucci, G. Ciani, D.M. Proserpio, Coord. Chem. Rev. 246 (2003) 247–289;
(c) L. Carlucci, G. Ciani, D.M. Proserpio, CrystEngComm. 5 (2003) 269–279;
(d) L. Carlucci, G. Ciani, D.M. Proserpio, S. Rizzato, Chem. Eur. J. 8 (2002) 1519–1526.
[4] (a) A.F. Wells, Structural Inorganic Chemistry, fifth ed., Oxford University Press, Oxford, 1984;
(b) A.F. Wells, Three-dimensional Nets and Polyhedra, Wiley, New York, 1977;
(c) A.F. Wells, Further Studies of Three-dimensional Nets, ACA Monograph, vol. 8, 1979.
[5] (a) J.V. Smith, Chem. Rev. 88 (1988) 149;
(b) J.V. Smith, Tetrahedral Frameworks of Zeolites, Clathrates and Related Materials, Landolt-Börnstein New Series IV/14 Subvolume A, Springer, Berlin, 2000.
[6] (a) M. O'Keeffe, B.G. Hyde, Crystal Structures I: Patterns and Symmetry, Washington, Mineral. Soc. Am., 1996;;
(b) M. O'Keeffe, M. Eddaoudi, H. Li, T. Reineke, O.M. Yaghi, J. Solid State Chem. 152 (2000) 152, 3–20;
(c) O. Delgado Friedrichs, M. O'Keeffe, O.M. Yaghi, Acta Crystallogr. A 59 (2003) 22–27;
(d) O. Delgado Friedrichs, M. O'Keeffe, O.M. Yaghi, Acta Crystallogr. A 59 (2003) 515–525;
(e) O. Delgado Friedrichs, M. O'Keeffe, O.M. Yaghi, Solid State Sci. 5 (2003) 73–78;
(f) O. Delgado Friedrichs, M. O'Keeffe, Acta Crystallogr. A 59 (2003) 351–360;
(g) C. Bonneau, O. Delgado Friedrichs, M. O'Keeffe, O.M. Yaghi, Acta Crystallogr. A 60 (2004) 517–520.
[7] (a) S.T. Hyde, S. Ramsden, Europhys. Lett. 50 (2000) 135–141;
(b) S.T. Hyde, C. Oguey, Eur. Phys. J. B 16 (2000) 613–630;

(c) S.T. Hyde, A.-K. Larsson, T. Di Matteo, S. Ramsden, V. Robins, Aust. J. Chem. 56 (2003) 981–1000;
(d) V. Robins, S. Ramsden, S.T. Hyde, Eur. Phys. J. B 39 (2004) 365–375;
(e) R. Nesper, S. Leoni, Chem. Phys. Chem. 2 (2001) 413–422;
(f) G. Thimm, Z. Kristallogr. 219 (2004) 528–536.

[8] M. Schindler, F.C. Hawthorne, W.H. Baur, Acta Crystallogr. B 55 (1999) 811–829.

[9] S.R. Batten, CrystEngComm. 3 (2001) 67.

[10] V.A. Blatov, A.P. Shevchenko, V.N. Serezhkin, J. Appl. Crystallogr. 33 (2000) 1193.

[11] More that a thousand of nets recognized by TOPOS are collected and described in detail at the website of M. O'Keeffe group at ASU, see http://okeeffe-ws1.la.asu.edu/RCSR/home.htm. Data on homogenous sphere packings come from Werner Fischer and Elke Koch and collaborators. 3-coordinated: E. Koch, W. Fischer, Z. Kristallogr. 210 (1995) 407–414; Cubic: W. Fischer, Z. Kristallogr. 138 (1973) 129–146; W. Fischer, Z. Kristallogr. 140 (1974) 50–74; W. Fischer, Z. Kristallogr. Acta Crystallogr. A 60 (2004) 246–249; W. Fischer, E. Koch, Acta Crystallogr. A 32 (1976) 225–232; Tetragonal: W. Fischer, Z. Kristallogr. 133 (1971) 18–42; W. Fischer, Z. Kristallogr. 194 (1991) 67–85, 87–110; W. Fischer, Z. Kristallogr. 205 (1993) 9–26; Hexagonal and trigonal: H. Sowa, E. Koch, Z. Kristallogr. 214 (1999) 316–323; H. Sowa, E. Koch, W. Fischer, Acta Crystallogr. A 59 (2003) 317–326; H. Sowa, E. Koch, Acta Crystallogr. A 60 (2004) 150–166; H. Sowa, E. Koch, Acta Crystallogr. A 60 (2004) 239–245; H. Sowa, E. Koch, Acta Crystallogr. A 61 (2005) 331–342; Triclinic: W. Fischer, E. Koch, Acta Crystallogr. A 58 (2002) 509–513. Other 4-coordinated structures: M. O'Keeffe, N.E. Brese, Acta Crystallogr. A 48 (1992) 663–669; M. O'Keeffe, Acta Crystallogr. A 48 (1992) 670–673; M. O'Keeffe, Acta Crystallogr. A 51 (1995) 916–920; M.M.J. Treacy, K.H. Randall, S. Rao, J.A. Perry, D.J. Chadi, Z. Kristallogr. 212 (1997) 768–791; M.M.J. Treacy, I. Rivin, E. Balkovsky, K.H. Randall, M.D. Foster, Microporous Mesop. Mater. 74 (2004) 121–132; M.D. Foster, O. Delgado Friedrichs, R.G. Bell, F.A.A. Paz, J. Klinowski, Angew. Chem. Int. Ed. 42 (2003) 3896–3899; J. Am. Chem. Soc. 126 (2004) 9769–9775. Other nets are from the enumerations of tilings: O. Delgado Friedrichs, A.W.M. Dress, D.H. Huson, J. Klinowsky, A.L. Mackay, Nature 400 (1999) 644–647; O. Delgado Friedrichs, D.H. Huson, Discrete Comput. Geom. 24 (2000) 279–292.

[12] In Class I all interpenetrated nets are related by symmetry translations $\boldsymbol{T}$ (either integral, or centering). In turn, all symmetry operations $\boldsymbol{W}$ relate atoms within the same net. However, one should keep in mind that the nets can also be transformed to each other by additional symmetry operations $\boldsymbol{WT} = \boldsymbol{TW}$. Further we will consider only the initial $\boldsymbol{T}$ and $\boldsymbol{W}$ motions ignoring their products for simplicity.

[13] In graph theory the number of edges incident on a vertex/node/site is called "degree", "coordination number" and also "valence". To keep consistence with the use of chemist and our previous works we prefer to use the term "connectivity", even if this term has a quite different meaning in the mathematics of graph theory. Thus, for a net in which vertices are of degree 3 and 4, we will use (3,4)-connected. Moreover the reader will find in the tables several examples where the nodes derived from *N*-coordinated metals) are of a degree less than *N*; e.g., 8-coordinated Sr in $Sr(AlCl_4)_2$ (56743) gives a 4-connected diamondoid topology. In all the tables when the chemical coordination is different from the connectivity/degree of the resulting node we will specify the former as N-coor (with oct for 6-coor). For a list of basic definitions used in graph theory see: J.W. Essam, M.E. Fisher, Rev. Mod. Phys. 42 (1970) 272.

[14] V.A. Blatov, L.V. Pogildyakova, V.N.Z. Serezhkin, Z. Kristallogr. 213 (1998) 202–209.

[15] V.A. Blatov, Cryst. Rev. 10 (2004) 249–318.

[16] A 'major' VDP face is a face crossed by a line passing through the two atoms separated by this face. Such atoms are called direct neighbors [see Ref. [14] and M. O'Keeffe, Acta Crystallogr. A 35 (1979) 772–775].

[17] V.N. Serezhkin, Yu.N. Mikhailov, Yu.A. Buslaev, Russ. J. Inorg. Chem. 42 (1997) 1871–1910.

[18] V.A. Blatov, Yu.A. Zakutkin, Z. Kristallogr. 217 (2002) 464–473.

[19] Ag_3BO_3:(26521) M. Jansen, W. Scheld, Z. Anorg. Allg. Chem. 477 (1981) 85–89;
$[(CO)_4Fe][Hg(SCN)]_2$: (68386) A.E. Mauro, R.H.A. Santos, M.T.P. Gambardella, R.H.P. Francisco, Polyhedron 6 (1987) 1273–1277;
$Ta(PS_4)S_2$: (23284) S. Fiechter, W.F. Kuhs, R. Nitsche, Acta Crystallogr. B 36 (1980) 2217–2220;
$HfTe_3O_8$: (9078) G. Meunier, J. Galy, Acta Crystallogr. B 27 (1971) 602–608;
$SnTe_3O_8$: (9077) G. Meunier, J. Galy, Acta Crystallogr. B 27 (1971) 602–608;
$TiTe_3O_8$: (98902) L. Bindi, C. Cipriani, Can. Mineral. 41 (2003) 1469–1473; (9076) G. Meunier, J. Galy, Acta Crystallogr. B 27 (1971) 602–608;
$ZrTe_3O_8$: (409713) O. Noguera, P. Thomas, O. Masson, J.-C. Champarnaud-Mesjard, Z. Kristallogr. New Cryst. Struct. 218 (2003) 293–294; (9079) G. Meunier, J. Galy, Acta Crystallogr. B 27 (1971) 602–608;
$K(GaTe_6O_{14})$: (280793) K.M. Ok, P.S. Halasyamani, Chem. Mater. 13 (2001) 4278–4284;
$(Hg_2)_3Cl_3O(OH)$: (71899) (71900) K. Mereiter, J. Zemann, A.W. Hewat, Am. Mineral. 77 (1992) 839–842; (12102) K. Mereiter, J. Zemann, Tschermaks Mineral. Petrogr. Mitt. 23 (1976) 105–115;
$CrP_3S_{9.238}$: (72596) P. Fragnaud, M. Evain, E. Prouzet, R. Brec, J. Solid State Chem. 102 (1993) 390–399;
$Ag_2(HgO_2)$: (280333) S. Deibele, J. Curda, E.-M. Peters, M. Jansen, Chem. Commun. (2000) 679–680;
$LiNa_2KFe_2Ti_2(Si_4O_{12})_2$: (34666) (35083) E. Cannillo, F. Mazzi, G. Rossi, Acta Crystallogr. 21 (1966) 200–208;
$Cs[AgZn(SCN)_4]$: (281130) M. Gunes, J. Valkonen, Acta Crystallogr. Sect. C-Cryst. Struct. Commun. 58 (2002) 161–163;
Ag(CNO): (66547) D. Britton, Acta Crystallogr. C 47 (1991) 2646–2647; (23833) D. Britton, J.D. Dunitz, Acta Crystallogr. 19 (1965) 662–668;
$NaTi_2(PS_4)_3$: (81997) X. Cieren, J. Angenault, J.-C. Couturier, S. Jaulmes, M. Quarton, F. Robert, J. Solid State Chem. 121 (1996) 230–235;
Ag_3BO_3: (32721) M. Jansen, G. Brachtel, Z. Anorg. Allg. Chem. 489 (1982) 42–46;
$Ta_2(P_2S_{11})$: (202397) M. Evain, S. Lee, M. Queignec, R. Brec, J. Solid State Chem. 71 (1987) 139–153.

[20] It is worth mention that using Systre [6f] this new (10^3) net does not give good embedding with equal edges. It may be consider to introduce extra vertices in the middle of longer edges (connected only to the 2 neighbours) to obtain realistic 3D embeddings.

[21] Cu_2O: (63281) R. Restori, D. Schwarzenbach, Acta Crystallogr. Sect. B 42 (1986) 201–208; (52043) A. Kirfel, K.D. Eichhorn, Acta Crystallogr. Sect. A 46 (1990) 271–284; (53322) Z.G. Pinsker, R.M. Imamov, Kristallografiya 9 (1964) 413–415; (38233) T. Yamaguti, Proc. Phys.: Math. Soc. Jpn. 20 (1938) 230–241; (26963) M.C. Neuburger, Z. Phys. 67 (1930) 845–850; (31057) P. Niggli, Z. Kristallogr. 57 (1922) 253–299;
Pd_2O: (77651)(57445) J. Kumar, R. Saxena, J. Less-Comm. Met. 147 (1989) 59–71;
Ag_2O: (281041) P. Norby, R.E. Dinnebier, A.N. Fitch, Inorg. Chem. 41 (2002) 3628–3637; (35540) R.W.G. Wyckoff, Am. J. Sci. 3 (1922) 184–188; (31058) P. Niggli, Z. Kristallogr. 57 (1922) 253–299;

Pb_2O: (28838) A. Ferrari, Gazz. Chim. It. 56 (1926) 630–637;
Zr_2O: (77714) V.I. Khitrova, V.V. Klechkovskaya, Kristallografiya 30 (1985) 70–73;
Au_2S: (78718) K. Ishikawa, T. Isonaga, S. Wakita, Y. Suzuki, Solid State Ion. 79 (1995) 60–66;
$Ag_{2-x}Au_xS$: (87215) (87216) (87217) J.C.W. Folmer, P. Hofman, G.A. Wiegers, J. Less-Comm. Met. 48 (1976) 251–268;
$Be(CN)_2$: (93725) D. Williams, B. Pleune, K. Leinenweber, J. Kouvetakis J. Solid State Chem. 159 (2001) 244–250;
$Cd(CN)_2$: (66938) B.F. Hoskins, R. Robson, J. Am. Chem. Soc. 112 (1990) 1546–1554; (20748) E.A. Shugam, G.S. Zhdanov, Zh. Fiz. Khim. 19 (1945) 515–518; (38117) E. Shugam, H. Zhdanov, Acta Physicochim. 20 (1945) 247–252;
$Mg(CN)_2$: (93726) D. Williams, B. Pleune, K. Leinenweber, J. Kouvetakis, J. Solid State Chem. 159 (2001) 244–250;
$Zn(CN)_2$: (412317) O. Reckeweg, A. Simon, Z. Naturforsch. (B) 57 (2002) 895–900; (22392) G.S. Zhdanov, Dokl. Akad. Nauk 31 (1941) 352–354; (66937) B.F. Hoskins, R. Robson, Am. Chem. Soc. 112 (1990) 1546–1554; (84968) (84967) D.J. Williams, D.E. Partin, F.J. Lincoln, J. Kouvetakis, M. O'Keeffe, J. Solid State Chem. 134 (1997) 164–169;
SiC_2N_4: (93543) R. Riedel, A. Greiner, G. Miehe, W. Dressler, H. Fuess, J. Bill, F. Aldinger, Angew. Chem. Int. Ed. Engl. 36 (1997) 603–606;
PtO_2: (77654) J. Kumar, R. Saxena, J. Less-Comm. Met. 147 (1989) 59–71;
$(NH_4)_3Cu_4Ho_2Br_{13}$: (78986) M.S. Wickleder, A. Bohnsack, G. Meyer, Z. Anorg. Allg. Chem. 622 (1996) 675–678;
$Rb_3Cu_4Tm_2Br_{13}$: (402503) A. Bohnsack, G. Meyer, Z. Kristallogr. New Cryst. Struct. 212 (1997) 1;
$(NH_4)_5Ce[Ni(NO_2)_6]_2$: (24541) A. Ferrari, L. Cavalca, M. Nardelli, Gazz. Chim. It. 81 (1951) 964–981;
$Ag(B(CN)_4)$: (411179) E. Bernhardt, G. Henkel, H. Willner, Z. Anorg. Allg. Chem. 626 (2000) 560–568;
$LiCo(CO)_4$: (30854) P. Kluefers, Z. Kristallogr. 167 (1984) 275–286;
$Ca(AlCl_4)_2$:(56730) P. Stegmueller, Dissertation Universitaet Karlsruhe, 1997, pp. 1–193;
$Yb(AlCl_4)_2$: (56729) P. Stegmueller, Dissertation Universitaet Karlsruhe, 1997, pp. 1–193;
$Sr(AlCl_4)_2$: (56727) (56728) P. Stegmueller, Dissertation Universitaet Karlsruhe, 1997, pp. 1–193; (56743) K. Mueller, Dissertation Universitaet Karlsruhe, 1993, pp. 1–158;
$CsHSO_4$: (77083) B.V. Merinov, Kristallografiya 42 (1997) 906–917; (63352) Z. Jirak, M. Dlouha, S. Vratislav, A.M. Balagurov, A.I. Beskrovnyi, V.I. Gordelii, I.D. Datt, L.A. Shuvalov, Phys. Status Solidi A 100 (1987) K117–K122; (73897) V. Varma, N. Rangavittal, C.N.R. Rao, J. Solid State Chem. 106 (1993) 164–173; (39253) Z. Nozik Yu, O.I. Lyakhovitskaya, N.M. Shchagina, V.A. Sarin, Kristallografiya 35 (1990) 658–660;
$CsDSO_4$: (62889) B.V. Merinov, A.I. Baranov, L.A. Shuvalov, B.A. Maksimov, Kristallografiya 32 (1987) 86–92; (62337) B.V. Merinov, A.I. Baranov, L.A. Shuvalov, B.A. Maksimov, Kristallografiya 32 (1987) 86–92;
$LiAlB_2O_5$: (51314) M. He, X.L. Chen, Y.C. Lan, H. Li, Y.P. Xu, J. Solid State Chem. 156 (1999) 181–184;
CdB_4O_7: (14361) M. Ihara, J. Krogh-Moe, Acta Crystallogr. 20 (1966) 132–134;
CoB_4O_7: (96560) J.L.C. Rowsell, N.J. Taylor, L.F. Nazar, J. Solid State Chem. 174 (2003) 189–197;
HgB_4O_7: (281287) M. Weil, Acta Crystallogr. Sect. E.: Struct Rep. Online 59 (2003) 40–42;
ZnB_4O_7: (9086) M. Martinez-Ripoll, S. Martinez-Carrera, S. Garcia-Blanco, Acta Crystallogr. B 27 (1971) 672–677; (23751) M. Martinez-Ripoll, S. Garcia-Blanco, An. Fisica 66 (1970) 209–210;
MnB_4O_7: (6170) S.C. Abrahams, J.L. Bernstein, P. Gibart, R.C. Sherwood, J. Chem. Phys. 60 (1974) 1899–1905;
MgB_4O_7: (34397) (34397) H. Bartl, W. Schuckmann, Neues Jahrb. Mineral. Monatsh. (1966) 142–148;
$Li_2B_4O_7$: (23876) J. Krogh-Moe, Acta Crystallogr. 15 (1962) 190–193; (65930) S.F. Radaev, L.A. Muradyan, L.F. Malakhova, Y.A. Burak, V.I. Simonov, Kristallografiya 34 (1989) 1400–1407; (300010) M. Natarajan-Iyer, R. Faggiani, I.D. Brown, Cryst. Struct. Commun. 8 (1979) 367–370; (34670) J. Krogh-Moe, Acta Crystallogr. B 24 (1968) 179–181;
CsB_5O_8: (93836) N. Penin, L. Seguin, M. Touboul, G. Nowogrocki, J. Solid State Chem. 161 (2001) 205–213;
KB_5O_8: (35486) J. Krogh-Moe, Arkiv foer Kemi 14 (1959) 439–449; (18192) J. Krogh-Moe, Acta Crystallogr. 18 (1965) 1088–1089; (2712) J. Krogh-Moe, Acta Crystallogr. B 28 (1972) 168–172;
RbB_5O_8: (93838) N. Penin, L. Seguin, M. Touboul, G. Nowogrocki, J. Solid State Chem. 161 (2001) 205–213; (92570) M.G. Krzhizhanovskaya, R.S. Bubnova, S.K. Filatov, A. Belger, P. Paufler, Z. Kristallogr. 215 (2000) 740–743;
TlB_5O_8: (50927) M. Touboul, G. Nowogrocki, J. Solid State Chem. 136 (1998) 216–220;
$Na_2B_6O_{10}$: (2045) J. Krogh-Moe, Acta Crystallogr. B 30 (1974) 747–752;
$Ag_2B_8O_{13}$: (98571) N. Penin, M. Touboul, G. Nowogrocki, Solid State Sci. 5 (2003) 559–564; (18134) J. Krogh-Moe, Acta Crystallogr. 18 (1965) 77–81;
$Na_2B_8O_{13}$: (95868) (95869) (95870) R.S. Bubnova, F. Shepelev Yu, N.A. Sennova, S.K. Filatov, Z. Kristallogr. 217 (2002) 444–450; (59748) N. Penin, M. Touboul, G. Nowogrocki, J. Solid State Chem. 168 (2002) 316–321; (14355) A. Hyman, A. Perloff, F. Mauer, S. Block, Acta Crystallogr. 22 (1967) 815–821;
BaB_8O_{13}: (26203) J. Krogh-Moe, M. Ihara, Acta Crystallogr. B 25 (1969) 2153–2154;
$Li_2(AlB_5O_{10})$: (279578) M. He, H. Li, X.-L. Chen, Y.-P. Xu, T. Xu, Acta Crystallogr. C 57 (2001) 1010–1011;
Ag_3CuS_2: (67526) C.L. Baker, F.J. Lincoln, A.W.S. Johnson, Austr. J. Chem. 45 (1992) 1441–1449;
$CsCo(CO)_4$: (31359) (31360) P. Kluefers, Z. Kristallogr. 165 (1983) 217–226.

[22] $[Ir_4(CO)_8F_2](Sb_2F_{11})_2$: (281482) I.-C. Hwang, K. Seppelt, Inorg. Chem. 42 (2003) 7116–7122.
$BeCl_2$: (78774) E. Spundflasche, H. Fink, H.J. Seifert, Z. Anorg. Allg. Chem. 621 (1995) 1723–1726; (92586) S.I. Troyanov, Zh. Neorg. Khim. 45 (2000) 1619–1624;
BeI_2: (92587) S.I. Troyanov, Zh. Neorg. Khim. 45 (2000) 1619–1624;
$ZnBr_2$: (30803) C. Chieh, M.A. White, Z. Kristallogr. 166 (1984) 189–197;
ZnI_2: (2404) P.H. Fourcroy, D. Carre, J. Rivet, Acta Crystallogr. B 34 (1978) 3160–3162;
HgI_2: (281134) M. Hostettler, D. Schwarzenbach, Acta Crystallogr. Sect. B: Struct. Sci. 58 (2002) 914–920;
GeS_2: (85527) M.J. MacLachlan, S. Petrov, R.L. Bedard, I. Manners, G.A. Ozin, Angew. Chem. Int. Ed. Engl. 37 (1998) 2076–2079;
$Be(NH_2)_2$: (34607) H. Jacobs, Z. Anorg. Allg. Chem. 427 (1976) 1–8;
$Mg(NH_2)_2$: (16222) H. Jacobs, Z. Anorg. Allg. Chem. 382 (1971) 97–109;
$Mn(NH_2)_2$: (89582) B. Froehling, G. Kreiner, H. Jacobs, Z. Anorg. Allg. Chem. 625 (1999) 211–216;
$Zn(NH_2)_2$: (89581) B. Froehling, G. Kreiner, H. Jacobs, Z. Anorg. Allg. Chem. 625 (1999) 211–216;
$Ca_3Ga_2N_4$: (86016) S.J. Clarke, F.J. DiSalvo, J. Alloys Compd. 274 (1998) 118–121;

$Na_2(SnAs_2)$: (73307) M. Asbrand, B. Eisenmann, Z. Naturforsch. B 48 (1993) 452–456;
$Li_5(B_7S_{13})$: (73150) F. Hiltmann, P. Zumhebel, A. Hammerschmidt, B. Krebs, Z. Anorg. Allg. Chem. 619 (1993) 293–302;
$Na_{5.88}B_{10}Se_{18}$: (412579) A. Hammerschmidt, A. Lindemann, M. Doech, B. Krebs, Solid State Sci. 4 (2002) 1449–1455;
$Na_6(B_{10}S_{18})$: (78993) A. Hammerschmidt, P. Zumhebel, F. Hiltmann, B. Krebs, Z. Anorg. Allg. Chem. 622 (1996) 76–84;
$Ag_6B_{10}S_{18}$: (33270) B. Krebs, H. Diercks, Z. Anorg. Allg. Chem. 518 (1984) 101–114;
$Li_{9.8}(B_{10}S_{18})S_{1.9}$: (69352) P. Zumhebel, B. Krebs, M. Gruene, W. Mueller-Warmuth, Solid State Ionics 43 (1990) 133–142;
$(Cd_4In_{16}S_{33})(H_2O)_{20}[(N_2C_4H_8)((NH_2)C_3H_6)_2]_{2.5}$: (93107) H.-L. Li, J. Kim, T.L. Groy, M. O'Keeffe, O.M. Yaghi, J. Am. Chem. Soc. 123 (2001) 4867–4868;
$(Zn_4In_{16}S_{33})[(N_2C_4H_8)((NH_2)C_3H_6)_2]$: (93103) C. Wang, Y.-Q. Li, X.-H. Bu, N.-F. Zheng, O. Zivkovic, C.-S. Yang, P.-Y Feng, J. Am. Chem. Soc. 123 (2001) 11506–11507;
$(Zn_4In_{16}S_{33})[(N_2C_4H_9)((NH_2)C_2H_4)]$: (93104) C. Wang, Y.-Q. Li, X.-H. Bu, N.-F. Zheng, O. Zivkovic, C.-S. Yang, P.-Y Feng, J. Am. Chem. Soc. 123 (2001) 11506–11507;
$(In_{2.39}Ge_{1.61}S_{33})[(H_2O)_{0.25}]$: (281747) N.-F. Zheng, X.-H. Bu, C. Wang, P.-Y. Feng, Science 298 (2002) 2366–2369.

[23] $Ce(IO_3)_4$: (20033) L.A. Azarova, E.E. Vinogradova, E.M. Mohajlova, V.I. Pakhomov, Dokl. Akad. Nauk SSSR 206 (1972) 613–615; (16665) D.T. Cromer, A.C. Larson, Acta Crystallogr. 9 (1956) 1015–1018;
Bi_4Rh: (58854) G.S. Zhdanov, Trudy Inst. Krist., Akad. Nauk SSSR 10 (1954) 99–116;
$KC(NO_2)_3$: (20483) N.I. Golovina, L.O. Atovmyan, Zh. Strukt. Khim. 8 (1967) 307–311;
$Ag_2Cs(B_{15}O_{24})$: (408026) A. Wiesch, K. Bluhm, Z. Naturforsch. B 53 (1998) 157–160;
$Zn[Au(CN)_2]_2$: (83675) B.F. Hoskins, R. Robson, N.V.Y. Scarlett, Angew. Chem. 107 (1995) 1317–1318;
$Co[Au(CN)_2]_2$: (41197) S.C. Abrahams, L.E. Zyontz, J.L. Bernstein, J. Chem. Phys. 76 (1982) 5458–5462;
$Ba(Nb_3O_6)$: (400773) S. Moehr, H. Mueller-Buschbaum, Z. Naturforsch. B 49 (1994) 915–918;
PBr_5: (22140) W. Gabes, K. Olie, Acta Crystallogr. B 26 (1970) 443–444; (15559) M. van Driel, C.H. MacGillavry, Recl. Trav. Chim. Pays-Bas Belg. 62 (1943) 167–171;
$NaCo(CO)_4$: (30855) P. Kluefers, Z. Kristallogr. 167 (1984) 275–286;
$(Se_6I)(SbF_6)$: (65837) W.A.S. Nandana, J. Passmore, P.S. White, C.M. Wong, Inorg. Chem. 28 (1989) 3320–3328;
$Mg[B(PO_4)(OH)_2](H_2O)_2$: (412922) H.-Z. Shi, Y.-K. Shan, M.-Y. He, Y.-Y. Liu, Z. Kristallogr.: New Cryst. Struct. 218 (2003) 21–22;
$(Ni_{0.5}Mg_{0.5})[B(PO_4)(OH)_2](H_2O)_2$: (411449) I. Boy, G. Schaefer, R. Kniep, Z. Anorg. Allg. Chem. 627 (2001) 139–143;
$Pb(PbF_6)$: (23467) P. Charpin, H. Marquet-Ellis, N.G.H.I. Nguyen, P. Plurien, C.R. Hebd. Seances Acad. Sci. Ser. C 275 (1972) 1503–1506;
$KBiF_6$: (25025) C. Hebecker, Z. Anorg. Allg. Chem. 384 (1971) 12–18;
$KNbF_6$: (16729) H. Bode, H. von Boehren, Acta Crystallogr. 11 (1958) 80–82;
$KSbF_6$: (42509) (632) G.J. Kruger, C.W.F.T. Pistorius, A.M. Heyns, Acta Crystallogr. B 3 (1976) 2916–2918;
$Ag(TaF_6)$: (411796) K. Matsumoto, R. Hagiwara, Y. Ito, O. Tamada, J. Fluorine Chem. 110 (2001) 117–122;
Tl_3VS_4: (200270) M. Vlasse, L. Fournes, C.R. Hebd. Seances Acad. Sci. Ser. C 287 (1978) 47–49; (16572) C. Crevecoeur, Acta Crystallogr. 17 (1964) 757;
Tl_3TaS_4: (16571) (16572) C. Crevecoeur, Acta Crystallogr. 17 (1964) 757;
Tl_3TaSe_4: (52431) C. Crevecoeur, Acta Crystallogr. 17 (1964) 757;
K_3SbS_4: (41895) (44676) H. Graf, H. Schaefer, Z. Anorg. Allg. Chem. 425 (1976) 67–80;
Na_3SbS_4: (44707) (76537) H. Graf, H. Schaefer, Z. Anorg. Allg. Chem. 425 (1976) 67–80;
Na_3SbSe_4: (65141) B. Eisenmann, R. Zagler, Z. Naturforsch. B 44 (1989) 249–256;
$K_2BaSnTe_4$: (80283) J. Li, H.-Y. Guo, D.M. Proserpio, A. Sironi, J. Solid State Chem. 117 (1995) 247–255.

[24] $[Co(H_2O)_4)_3(W_6S_8(CN)_6)(H_2O)_{23.13}$: (281147) S. Jin, F.J. Disalvo, J. Biochem. 14 (2002) 3448–3457;
$[Fe(H_2O)_4]_3(W_6S_8(CN)_6)(H_2O)_{24.62}$: (281146) S. Jin, F.J. Disalvo, J. Biochem. 14 (2002) 3448–3457;
$[Mn(H_2O)_4)_3(W_6S_8(CN)_6)(H_2O)_{23.4}$: (281145) S. Jin, F.J. Disalvo, J. Biochem. 14 (2002) 3448–3457;
La_2O_3: (44692) P. Aldebert, J.P. Traversse, Mater. Res. Bull. 14 (1979) 303–323;
Nd_2O_3: (100216) P. Aldebert, J.P. Traversse, Mater. Res. Bull. 14 (1979) 303–323;
$[Co(H_2O)_4]_3(V_{18}O_{42}(SO_4)_{0.5}(VO_4)_{0.5})(H_2O)_{24}$: (410239) M.I. Khan, E. Yohannes, R.J. Doedens, Angew. Chem. Int. Ed. Engl. 38 (1999) 1292–1294;
$[Fe(H_2O)_4]_3(V_{18}O_{42}(SO_4)_{0.5}(VO_4)_{0.5})(H_2O)_{24}$: (410238) M.I. Khan, E. Yohannes, R.J. Doedens, Angew. Chem. Int. Ed. Engl. 38 (1999) 1292–1294;
$(N_2H_5)_2(Mg_3(H_2O)_{12}V_{18}O_{42}(V_xS_{1-x}O_4))(H_2O)_{24}$: (411144) M.I. Khan, E. Yohannes, R.J. Doedens, S. Tabussum, S. Cevik, L. Manno, D. Powell, Cryst. Eng. 2 (1999) 171–179;
$Li_6(Mn_3(H_2O)_{12}V_{18}O_{42}(V_xS_{1-x}O_4))\cdot(H_2O)_{24}$: (411145) M.I. Khan, E. Yohannes, R.J. Doedens, S. Tabussum, S. Cevik, L. Manno, D. Powell, Cryst. Eng. 2 (1999) 171–179;
$Co[Ag(CN)_2]_3$: (16959) A. Ludi, H.U. Guedel, Helv. Chim. Acta 51 (1968) 1762–1765; (28501) L. Pauling, P. Pauling, Proc. Natl. Acad. Sci. USA 60 (1968) 362–367;
$K_2Na[Ag(CN)_2]_3$: (65699) M. Zabel, S. Kuehnel, K.-J. Range, Acta Crystallogr. C 45 (1989)1619–1621;
$KMn[Ag(CN)_2]_3$: (281280) U. Geiser, J.A. Schlueter, Acta Crystallogr. C 59 (2003) 21–23;
$RbCd[Ag(CN)_2]_3$: (75503) B.F. Hoskins, R. Robson, N.V.Y. Scarlett, J. Chem. Soc. Chem. Commun. (1994) 2025–2026;
$KCo[Au(CN)_2]_3$: (201056) S.C. Abrahams, J.L. Bernstein, R. Liminga, E.T. Eisenmann, J. Chem. Phys. 73 (1980) 4585–4590;
$H_6Mn_3[V_{19}O_{46}(H_2O)_{12}](H_2O)_{30}$: (87982) M.I. Khan, E. Yohannes, D. Powell, Inorg. Chem. 38 (1999) 212–213;
$Li_9B_{19}S_{33}$: (73151) F. Hiltmann, P. Zumhebel, A. Hammerschmidt, B. Krebs, Z. Anorg. Allg. Chem. 619 (1993) 293–302;
$Fe(OH)Te_2O_5$: (100139) F. Pertlik, A. Gieren, Neues Jahrb. Mineral. Monatsh. (1977) 145–154; (16998) F. Pertlik, Anz. Oesterr. Akad. Wiss. Math.: Naturwiss. Kl. 105 (1968) 332–333; (4439) F. Pertlik, Tschermaks Mineral. Petrogr. Mitt. 13 (1969) 219–232;
Nb_6F_{15}: (25769) H. Schaefer, H.G. von Schnering, K.J. Niehues, H. Nieder Vahrenholz, J. Less-Comm. Met. 9 (1965) 95–104;
$Th_6H_7Br_{15}$: (69053) A. Simon, F. Boettcher, J.K. Cockroft, Angew. Chem. 103 (1991) 79–80; (33928) F. Boettcher, A. Simon, R.K. Kremer, H. Buchkremer-Hermanns, J.F. Cockcroft, Z. Anorg. Allg. Chem. 598 (1991) 25–44;
$Th_6D_7Br_{15}$: (69054) A. Simon, F. Boettcher, J.K. Cockroft, Angew. Chem. 103 (1991) 79–80; (33929) F. Boettcher, A. Simon, R.K. Kremer, H. Buchkremer-Hermanns, J.F. Cockcroft, Z. Anorg. Allg. Chem. 598 (1991) 25–44;
Zr_6CoCl_{15}: (71148) J. Zhang, J.D. Corbett, Inorg. Chem. 30 (1991) 431–435;

Zr_6NiCl_{15}: (71149) J. Zhang, J.D. Corbett, Inorg. Chem. 30 (1991) 431–435;
$CoTh_6Br_{15}$: (33926) F. Boettcher, A. Simon, R.K. Kremer, H. Buchkremer-Hermanns, J.K. Cockcroft, Z. Anorg. Allg. Chem. 598 (1991) 25–44;
$FeTh_6Br_{15}$: (33925) F. Boettcher, A. Simon, R.K. Kremer, H. Buchkremer-Hermanns, J.K. Cockcroft, Z. Anorg. Allg. Chem. 598 (1991) 25–44;
$NaFeTh_6Br_{15}$: (33927) F. Boettcher, A. Simon, R.K. Kremer, H. Buchkremer-Hermanns, J.K. Cockcroft, Z. Anorg. Allg. Chem. 598 (1991) 25–44;
$Li_2Zr_6MnCl_{15}$: (71146) J. Zhang, J.D. Corbett, Inorg. Chem. 30 (1991) 431–435;
$Li_2Zr_6FeCl_{15}$: (71147) J. Zhang, J.D. Corbett, Inorg. Chem. 30 (1991) 431–435;
$Eu[Ag(CN)_2]_3(H_2O)_3$: (81234) Z. Assefa, R.J. Staples, J.P. Fackler Jr., H. Patterson, G. Shankle, Acta Crystallogr. C 51 (1995) 2527–2529.

[25] The high-symmetry **acs** topology has been recently identified as the default arrangement for linking trigonal prisms together. A.C. Sudik, A.P. Côté, Omar M. Yaghi, Inorg. Chem. 44 (2005) 2998–3000, and references therein.

[26] $Cs(B_9O_{14})$: (99793) A.C. Wright, R.N. Sinclair; C.E. Stone, K.S. Knight, I.G. Polyakova, N.M. Vedishcheva, B.A. Shakhmatkin, Phys. Chem. Glasses 44 (2003) 197–202; (97512) N. Penin, M. Touboul, G. Nowogrocki, J. Solid State Chem. 175 (2003) 348–352; (15331) J. Krogh-Moe, M. Ihara, Acta Crystallogr. 23 (1967) 427–430;
Ag_2HgS_2: (201713) J.-J. Guillou, J. Monthel, P. Picot, F. Pillard, J. Protas, J.-C. Samama, Bull. Mineral. 108 (1985) 457–464;
$Hg_2[B(CN)_4]_2$: (412298) M. Berkei, E. Bernhardt, M. Schuermann, M. Mehring, H. Willner, Z. Anorg. Allg. Chem. 628 (2002) 1734–1740;
Hg_3OCl: (89686) N.V. Pervukhina, G.V. Romanenko, S.A. Magarill, V.I. Vasiliev, S.V. Borisov, J. Struct. Chem. 40 (1999) 155–158; (87734) V.I. Vasiliev, N.V. Pervukhina, G.V. Romanenko, S.A. Magarill, S.V. Borisov, Can. Mineral. 37 (1999) 119–126;
$Cu_2(Mo_6Cl_{14})$: (404375) A. Peppenhorst, H.-L. Keller, Z. Anorg. Allg. Chem. 622 (1996) 663–669;
$Cu_2(W_6Cl_{14})$: (409272) Y.-Q. Zheng, J. Nuss, H.G. von Schnering, Z. Kristallogr. New Cryst. Struct. 213 (1998) 680;
$Cu_2(Mo_6Br_{14})$: (404376) A. Peppenhorst, H.-L. Keller, Z. Anorg. Allg. Chem. 622 (1996) 663–669;
$Cu_2(W_6Br_{14})$: (83581) S. Ihmaine, C. Perrin, M. Sergent, Eur. J. Solid State Inorg. Chem. 34 (1997) 169–178; (408569) Y.-Q. Zheng, Y. Grin, K. Peters, H.G.V. Schnering, Z. Anorg. Allg. Chem. 624 (1998) 959–964;
$[Zn(H_2O)]_2\{S_8[Re(CN)]_6\}(H_2O)_7$: (86652) L.G. Beauvais, M.P. Shores, J.R. Long, Chem. Mat. 10 (1998) 3783–3786;
$Pd_{13}Cu_3S_7$: (32054) P. Matkovic, M. El Boragy, K. Schubert, J. Less-Comm. Met. 50 (1976) 165–176;
$Pd_{16}S_7$: (77887) C. Romming, E. Roest, Acta Crystallogr. A 30 (1976) 425–428; (32053) P. Matkovic, M. El Boragy, K. Schubert, J. Less-Comm. Met. 50 (1976) 165–176.

[27] γ-MnO_2: (78331) C. Fong, B.J. Kennedy, M.M. Elcombe, Z. Kristallogr. 209 (1994) 941–945.

[28] Ta_4PS_{29}: (201659) M. Evain, M. Queignec, R. Brec, J. Rouxel, J. Solid State Chem. 56 (1985) 148–157;
$LiNa_2K(Fe_{1.63}Mg_{0.37})(Si_4O_{12})_2$: (71358–71361) M. Kunz, T. Armbruster, G.A. Lager, A.J. Schultz, R.J. Goyette, W. Lottermoser, G. Amthauer, Phys. Chem. Miner. 18 (1991) 199–213;
$K_4[Pd(Se_4)_2][Pd(Se_6)_2]$: (71947) K.-W. Kim, M.G. Kanatzidis, J. Am. Chem. Soc. 114 (1992) 4878–4883;
$Hg_3CdCl_2(SCN)_6$: (412499) A. Mosset, M. Bagieu-Beucher, A. Lecchi, R. Masse, J. Zaccaro, Solid State Sci. 4 (2002) 827–834;
Li_2Pd_3B: (84931) U. Eibenstein, W. Jung, J. Solid State Chem. 133 (1997) 21–24;
$Bi_3GaSb_2O_{11}$: (10172) A.W. Sleight, R.J. Bouchard, Inorg. Chem. 12 (1973) 2314–2316;
$Bi_3AlSb_2O_{11}$: (82633) (82634) Ismunandar, B.J. Kennedy, B.A. Hunter, J. Solid State Chem. 127 (1996) 178–185; (87109–87115) Ismunandar, B.J. Kennedy, B.A. Hunter, Solid State Commun. 108 (1998) 649–654;
$La_3Ru_3O_{11}$: (100517) F. Abraham, J. Trehoux, D. Thomas, Mater. Res. Bull. 13 (1978) 805–810;
$La_3Ir_3O_{11}$: (200472) F. Abraham, J. Trehoux, D. Thomas, J. Less-Comm. Met. 63 (1979) 57–63;
$Bi_3Ru_3O_{11}$: (24955) F. Abraham, D. Thomas, G. Novogorocki, Bull. Soc. Fr. Mineral. Crystallogr. 98 (1975) 25–29; (74382) G.R. Facer, M.M. Elcombe, B.J. Kennedy, Aust. J. Chem. 46 (1993) 1897–1907;
$NaBi_2Sb_3O_{11}$: (79859) J.-C. Champarnaud-Mesjard, B. Frit, A. Aftati, M. El Farissi, Eur. J. Solid State Inorg. Chem. 32 (1995) 495–504;
$[Ho_2(Pb_4O_4)](Al_6O_{12})$: (67819) M. Scheikowski, H. Mueller-Buschbaum, Z. Anorg. Allg. Chem. 619 (1993) 1755–1758;
$[Lu_2(Pb_4O_4)](Al_6O_{12})$: (67820) M. Scheikowski, H. Mueller-Buschbaum, Z. Anorg. Allg. Chem. 619 (1993) 1755–1758;
$[Eu_2(Pb_4O_4)](Al_6O_{12})$: (404478) H.K. Mueller-Buschbaum, J.-P. Werner, Z. Naturforsch. B 51 (1996) 883–887;
$[Gd_2(Pb_4O_4)](Al_6O_{12})$: (404479) H.K. Mueller-Buschbaum, J.-P. Werner, Z. Naturforsch. B 51 (1996) 883–887;
$[Nd_2(Pb_4O_4)](Al_6O_{12})$: (406531) H.K. Mueller-Buschbaum, J.-P. Werner, Z. Naturforsch. B 52 (1997) 449–452;
$[Sm_2(Pb_4O_4)](Al_6O_{12})$: (406532) H.K. Mueller-Buschbaum, J.-P. Werner, Z. Naturforsch. B 52 (1997) 449–452.

[29] $(H_3O)(SbF_6)$: (66552) E.M. Larson, K.D. Abney, A.C. Larson, P.G. Eller, Acta Crystallogr. B 47 (1991) 206–209;
NH_2CN: (40446) L. Denner, P. Luger, J. Buschmann, Acta Crystallogr. C 44 (1988) 1979–1981
$[C(NH_2)_3]Cl$: (23835) D.J. Haas, D.R. Harris, H.H. Mills, Acta Crystallogr. 19 (1965) 676–679;
$H_2Te_2O_3F_4$: (9653) J.C. Jumas, M. Maurin, E. Philippot, J. Fluor. Chem. 8 (1976) 329–340;
$\{Cu[CS(NH_2)_2]_3\}Cl$: (281646) P. Bombicz, I. Mutikainen, M. Krunks, T. Leskela, J. Madarasz, L. Niinisto, Inorg. Chim. Acta 357 (2004) 513–525; (16580) Y. Okaya, C.B. Knobler, Acta Crystallogr. 17 (1964) 928–930;
$\{Cu[CS(NH_2)_2]_3\}Br$: (281647) P. Bombicz, I. Mutikainen, M. Krunks, T. Leskela, J. Madarasz, L. Niinisto, Inorg. Chim. Acta 357 (2004) 513–525;
NH_4Br: (43300) V.N. Kolomiichuk, V.F. Dvoryankin, Kristallografiya 9 (1964) 50–56;
NH_4I: (22154) V. Hovi, K. Paavola, E. Nurmi, Ann. Acad. Sci. Fenn. Ser. A 6: Physica 328 (1969) 1–8;
H_2O Ice VII: (31868) B. Kamb, B.L. Davis, Proc. Natl. Acad. Sci. USA 52 (1964) 1433–1439;
D_2O Ice VII (64773) (64774) J.D. Jorgensen, T.G. Worlton, J. Chem. Phys. 83 (1985) 329–333; (201701) W.F. Kuhs, J.L. Finney, C. Vettier, D.V. Bliss, J. Chem. Phys. 81 (1984) 3612–3623;
D_2O Ice VIII: (44102) (44103) (44104) J.M. Besson, P. Pruzan, S. Klotz, G. Hamel, B. Silvi, R.J. Nelmes, J.S. Loveday, R.M. Wilson, S. Hull, Phys. Rev. B 49 (1994) 12540–12550; (49809) (201700) W.F. Kuhs, J.L. Finney, C. Vettier, D.V. Bliss, J. Chem. Phys. 81 (1984) 3612–3623; (201703) J.D. Jorgensen, R.A. Beyerlein, R.A. Watanabe, T.G. Worlton, J. Chem. Phys. 81 (1984) 3211–3214;
$(D_2O)_2(DF)_3$: (67267) W. Poll, M. Lohmeyer, D. Mootz, Z. Naturforsch. B 44 (1989) 1359–1364;
$(NH_4)(IO_4)$: (280083) W. Levason, M. Webster, Acta Crystallogr. C 55(6) (1999); (52341) J. Beintema, Strukturbericht 3 (1937)

421–423; (52379) H. Braekken, Norsk Videnskab Selskab Forh. 1 (1928) 149–152;
$(ND_4)(IO_4)$: (23280) R.J.C. Brown, S.L. Segel, Acta Crystallogr. B 36 (1980) 2195–2198;
$(NH_4)(ReO_4)$: (1394) (1395) G.J. Kruger, E.C. Reynhardt, Acta Crystallogr. B 34 (1978) 259–261;
$(ND_4)(ReO_4)$: (77923) I.P. Swainson, R.J.C. Brown, Acta Crystallogr. Sect. B: Struct. Sci. 53 (1997) 78–81; (23278) (23279) R.J.C. Brown, S.L. Segel, Acta Crystallogr. B 36 (1980) 2195–2198; (72964) (72966) (72968) B.M. Powell, R.J.C. Brown, A.M. Harnden, J.K. Reid, Acta Crystallogr. B 49 (1993) 463–468;
$NH_4[F(HF)_3]$: (38337) D. Mootz, W. Poll, Z. Naturforsch. B 39 (1984) 290–297;
$[Cd((NH_2)_2CS)_4]Cl_2$: (92579) X.N. Jiang, W.T. Yu, D.R. Yuan, D. Xu, M.K. Lu, X.Q. Wang, S.Y. Guo, M.H. Jiang, Z. Krist.: New Cryst. Struct. 215 (2000) 499–500;
H_2S IV h.p.: (50333) H. Fujihisa, H. Yamawaki, M. Sakashita, K. Aoki, S. Sasaki, H. Shimizu, Phys. Rev. B 57 (1998) 2651–2654;
$Rb(H_2C_6N_9)(H_2O)_{0.5}$: (413139) B. Juergens, H.A. Hoeppe, W. Schnick, Z. Anorg. Allg. Chem. 630 (2004) 35–40;
$(NH_4)[N(CN)_2]$: (413097) B.V. Lotsch, J. Senker, W. Kockelmann, W. Schnick, J. Solid State Chem. 176 (2003) 180–191;;
$(ND_4)[N(CN)_2]$: (281696) B.V. Lotsch, J. Senker, W. Schnick, Inorg. Chem.43 (2004) 895–904; (97581) B.V. Lotsch, J. Senker, W. Kockelmann, W. Schnick, J. Solid State Chem. 176 (2003) 180–191;
$(NH_4)[N(NO_2)_2]$: R. Gilardi, J. Flippen-Anderson, C. George, R.J. Butcher, J. Am. Chem. Soc. 119 (1997) 9411–9416;
$HCl(H_2O)_2$: (15353) (15353) J.O. Lundgren, I. Olovsson, Acta Crystallogr. 23 (1967) 966–971;
$HBr(H_2O)_2$: (34105) R. Attig, J.M. Williams, Angew. Chem. 88 (1976) 507–508;
H_2O Ice VI: (16950) B. Kamb, Science 150 (1965) 205–209;
D_2O Ice VI: (201702) W.F. Kuhs, J.L. Finney, C. Vettier, D.V. Bliss, J. Chem. Phys. 81 (1984) 3612–3623;
NH_4HF_2: (14140) T.R.R. McDonald, Acta Crystallogr. 13 (1960) 113–124; (28893) M.T. Rogers, L. Helmholz, J. Am. Chem. Soc. 62 (1940) 1533–1536;
NH_4N_3: (412211) H.-W. Lerner, M. Bolte, N. Wiberg, J. Organomet. Chem. 649 (2002) 246–251; (2236) E. Prince, C.S. Choi, Acta Crystallogr. B 34 (1978) 2606–2608; (20751) Z.V. Zvonkova, G.S. Zhdanov, Zh. Fiz. Khim. 23 (1949) 1495–1501;
$(NH_4)(NO_3)$: (37128) C.S. Choi, H.J. Prask, Acta Crystallogr. B 39 (1983) 414–420;
$(ND_4)(NO_3)$: (35435) M. Ahtee, K.L. Smolander, B.W. Lucas, A.W. Hewat, Acta Crystallogr. C 39 (1983) 651–655; (35775) M. Ahtee, K.J. Smolander, B.W. Lucas, A.W. Hewat, Acta Crystallogr. B 39 (1983) 685–687; (37127) C.S. Choi, H.J. Prask, Acta Crystallogr. B 39 (1983) 414–420;
$(NH_4)_6(MnMo_9O_{32})(H_2O)_6$: (67575) H. Stratemeier, M.A. Hitchman, D.L. Kepert, B.W. Skelton, K.E. Sugars, A.H. White, J. Chem. Soc. Dalton Trans. (1992) 3035–3039;
$(NH_4)_6(NiMo_9O_{32})(H_2O)_6$: (49909) T.J. Weakley, Acta Crystallogr. 43 (1987) 2221–2222;
$LiNa_2H[Al(PO_4)_2(OH)]$: (31274) F.C. Hawthorne, Tschermaks Mineral. Petrogr. Mitt. 31 (1983) 121–135;
$H_3(Co(CN)_6$: (2862) R. Haser, C.E. de Broin, M. Pierrot, Acta Crystallogr. B 28 (1972) 2530–2537; (28502) L. Pauling, P. Pauling, Proc. Natl. Acad. Sci. USA 60 (1968) 362–367; (16958) H.U. Guedel, A. Ludi, H. Buerki, Helv. Chim. Acta 51 (1968) 1383–1389;
$D_3Co(CN)_6$: (9484) H.U. Guedel, A. Ludi, J. Chem. Phys. 56 (1972) 674–675; (9487) H.U. Guedel, A. Ludi, J. Chem. Phys. 53 (1970) 1917–1923;
$H_3Fe(CN)_6$: (2861) R. Haser, C.E. de Broin, M. Pierrot, Acta Crystallogr. B 28 (1972) 2530–2537.

[30] G.R. Desiraju, T. Steiner, The Weak Hydrogen Bond, Oxford University Press, Oxford, 1999.